DMD Fast Forward. Published on December 12, 2008 as doi:10.1124/dmd.108.024364

Title page

Investigation of the *in vitro* metabolism of the analgesic flupirtine

Karen Methling, Przyemsław Reszka, Michael Lalk, Oldrich Vrana, Eberhard Scheuch, Werner Siegmund, Bernd Terhaag and Patrick J. Bednarski*

Institute of Pharmacy, University of Greifswald, 17487 Greifswald, Germany (KM, PR, ML, PJB) (primary laboratory)

Institute of Biophysics, Academy of Sciences of the Czech Republic, v.v.i., 61265 Bruno, Czech Republic (OV)

Institute of Pharmacology, University of Greifswald, 17487 Greifswald, Germany (ES, WS)

AWD.pharma GmbH & Co. KG Wasa Str. 50, 01445 Radebeul, 01097 Dresden, Germany (BT)

*Corresponding author

Running title page

a) In vitro metabolism of flupirtine

b) Patrick J. Bednarski, Institut für Pharmazie, Universität Greifswald, 17487 Greifswald, Germany. Tel. ++49 3834 86 48 83. FAX ++49 3834 86 48 02. email bednarsk@uni-greifswald.de.

Number of text pages: 28
Number of tables: 3
Number of figures: 8
Number of schemes: 7
Number of references: 38
Number of words in Abstract: 246
Number of words in Introduction: 673
Number of words in Discussion: 1865

Abbreviations: COX: cyclooxygenase, CV: cyclic voltammetry, CYP: cytochrome P450, DAD: diode array detector, GCE: glassy carbon electrode, GSH: reduced glutathione, IU: international units, HPLC: high performance liquid chromatography, HRMS: high resolution mass spectrometry, HRP: horse radish peroxidase, MAO: monoamine oxidase, MPO: myeloperoxidase, NADPH: reduced nicotinamide adenine dinucleotide phosphate, NAT: *N*-acetyltransferase, POD: peroxidase, UGT: UDP-glucuronosyltransferase, UDPGA: uridine 5'-diphosphoglucuronic acid.

DMD Fast Forward. Published on December 12, 2008 as DOI: 10.1124/dmd.108.024364
This article has not been copyedited and formatted. The final version may differ from this version.

Abstract

The *in vitro* metabolism of flupirtine, ethyl-*N*-[2-amino-6-(4-fluoro-phenylmethyl-amino)pyridine-3-yl]carbamate, a centrally acting analgesic with muscle tone reducing activity, was studied. Two flupirtine metabolites were already known: the *N*-acetylated analogue D13223 and 4-fluorohippuric acid. The structure of flupirtine suggested that redox chemistry may play a role in metabolism and cyclic voltammery studies showed that the drug undergoes facile and irreversible redox reactions. Thus, oxidative metabolism was investigated first. With CYP3A1-induced rat liver microsomes an 18% turnover of flupirtine and a 20-25% turnover of D13223 took place over 30 min but less than 5% turnover of flupirtine was observed with all human liver microsomal preparations tested, evidence that CYP450 does not contribute appreciably to the metabolism in humans. Likewise, no involvement of human monoamine oxidase (isoforms A and B) was found for either flupirtine or D13223. In contrast, flupirtine was an excellent substrate for both human myeloperoxidase and horse radish peroxidise (HRP). These enzymes produced detectable amounts of oxidation products. Incubations of flupirtine with HRP produced an oxidation product that could be trapped with GSH, the resulting glutathione conjugate was characterized by MS and NMR. Metabolism of D13223 by both peroxidases was also observed but to a much lesser extent. Porcine liver esterases cleave the carbamate group of flupirtine and both human *N*-acetyltransferases 1 and 2 acetylated the hydrolysis product, presumably descarboethoxyflupirtine, with nearly equal efficiencies to yield D13223. Incubations of human liver microsomes with flupirtine or the metabolite D13223 together with UDPGA gave two isomeric *N*-glucuronides in both cases.

Introduction

Flupirtine (**1**) maleate (ethyl-*N*-[2-amino-6-(4-fluoro-phenylmethylamino)pyridin-3-yl]carbamate maleate, Katadolon®) (Scheme 1), a centrally acting non-opiate analgesic with muscle tone reducing activity, does not show the classical side-effects of opiates or non-steroidal anti-inflammatory analgesics (Jakovlev et al, 1985; Szelenyi and Nickel, 1991). The drug has been effectively and safely used in Germany for 20 years. The mode of action is now mostly understood. Modification of prostaglandin formation is of minor importance for the analgesic action of flupirtine. (Darius and Schrör, 1985) Evidence has accumulated that flupirtine interacts indirectly with the NMDA-responsive subtype of the glutamate receptor, possibly by opening K^+ channels (Kornhuber et al, 1999a, Kornhuber et al 1999b, Jakob and Krieglstein, 1997) Clinical interest in the compound is growing as further indications for the drug are found. For example, successful treatment of fibromyalgia has been reported (Stoll, 2000). In particular, the neuroprotective properties attributed to flupirtine are making it a possible candidate for treatment of Parkinson's and Alzheimer's diseases, Creutzfeld-Jacob-Disease (CJD) and other neurodegenerative aliments (Schuster et al. 1998; Schröder and Müller, 2002; Otto et al., 2004).

SCHEME 1

Relatively little has been reported on the metabolism of flupirtine. Initial pharmacokinetic investigations in the 1980s reported two metabolites, the *N*-acetylated analogue D13223 (**2**) (Scheme 1) and 4-fluorohippuric acid. Both were found in the urine of rats, dogs (Obermeier et al., 1985) and humans (Hlavica and Niebch, 1985) administered oral or intravenous flupirtine. These studies used ^{14}C-labled flupirtine to characterize and quantify metabolism. In urine of humans 0-8 h following an oral dose of flupirtine, ca. 20% of the total dose was found to be D13223, 20% was 4-fluorohippuric acid and ca. 15% was parent drug. (Hlavica and Niebch, 1985) At that time, various hydrophilic and unstable metabolites were

also detected, in particularly in the bile of rats and dogs, but structural characterisations of these metabolites were not reported. (Obermeier et al., 1985) These authors postulated, however, that the hydrophilic metabolites were unlikely to be glucuronide or sulphate conjugates because they were not cleavable with the appropriate enzymes. In these early studies no data were published on the possible role of phase I or phase II enzymes and the pathways of flupirtine metabolism.

The desaza analogue of flupirtine, retigabine (**3**) (ethyl-*N*-[2-amino-4-(4-fluoro-phenylmethylamino)phenyl]carbamate, shows pronounced anticonvulsant activities in a variety of animal models (Tober et al., 1996; Rostock et al., 1996), and is currently under clinical investigation for the treatment of epileptic seizures. In contrast to flupirtine, the *in vitro* metabolism of retigabine has been extensively studied. *In vitro* incubations of retigabine with human liver slices and microsomes did not show a contribution by cytochrome P450 monooxygenase (CYP) in the phase I metabolism of the drug. On the other hand, retigabine in the presence of microsomes and uridine 5'-diphosphoglucuronic acid (UDPGA) reacted to form two *N*-glucuronides (McNeilly et al., 1997; Hiller et al., 1999; Borlak et al., 2006). In fact, the *in vivo* metabolism of retigabine is dominated by these glucuronidation reactions, and structures of the two regioisomeric *N*-glucuronides have been determined (Hiller et al., 1999; Hempel et al., 1999; Borlak et al., 2006). For retigabine the *N*-acetyl metabolite, analogous to the flupirtine metabolite D13223, was also detected in urine and plasma from rats and humans (Hempel et al., 1999). This metabolite was also detected in incubations with rat and human liver slices. However, reaction pathways for the cleavage of the carbamate residue and the *N*-acetylation reaction were not investigated.

The aim of the present work was to characterize in more detail the *in vitro* metabolism of flupirtine to help predict new metabolites in preparation for a detailed clinical pharmacokinetic study. The structure of flupirtine suggested that redox reactions involving the pyridine triamino structure might be important. The potential roles of various oxidative

enzymes such as CYP, monoamine oxidases (MAO) and peroxidases in phase I metabolism were investigated. Furthermore, hydrolysis reactions and conjugation reactions with acetate, glutathione (GSH) and glucuronic acid have been studied as possible phase II pathways. Characterization of the metabolites has been carried out by HPLC, LC-HRMS, LC-MS/MS, MS/MS and NMR methods.

Materials and Methods

Chemicals and enzymes. Flupirtine maleate ($C_{15}H_{17}FN_4O_2 \cdot C_4H_4O_4$) and D13223 ($C_{14}H_{15}FN_4O$) were obtained from AWD.pharma GmbH & Co. KG (Radebeul, Germany). (Seydel et al., 1994) UDP-glucuronic acid, desferoxamine, glutathione (reduced form), horse radish peroxidase (HRP), human myeloperoxidase (MPO), acetyl-CoA, acetyl-*d,l*-carnitine, carnitine acetyl transferase, monoamine oxidase A and B (MAO A, B; recombinant, expressed in Baculovirus infected BTI insect cells) and MAO insect cell control were all purchased from Sigma (Taufkirchen, Germany). Porcine liver esterase was from Fluka (Taufkirchen, Germany) and human recombinant *N*-acetyltransferases 1 and 2 were from BD Bioscience (Franklin Lakes, NJ). All other chemicals came from commercial suppliers in analytical grade. HPLC gradient grade acetonitrile and methanol were purchased from J. T. Baker (Phillipsburg, NJ) or VWR (Leuven, Belgium).

Microsomes and S9-fractions. Rat liver microsomes and S9-fractions were prepared by standard procedures (Walter et al., 2003) and stored at - 32 °C. The human liver microsomes and S9-fractions were purchased from InVitro Technologies, Inc. (Baltimore, MD, USA) and stored at –70 °C.

Cyclic voltammetry. Solutions of flupirtine and D13223 were prepared in 0.1 M Tris-HCl buffer (pH 7.4). The concentration of both analytes was adjusted to 1 mM by checking the absorbance at λ = 318 nm (ε = 3,970 and 4,140 M^{-1} cm for flupirtine and D13223,

respectively). The solutions were analyzed within 24 h of dissolution. (The solutions exhibited identical spectra within 1 month of storage in the dark at 4 °C.) An Electrochemical Analyzer Autolab PG Stat 302 with glassy carbon electrode (GCE) (diameter was 3.1 mm), was used with a three-electrode system GCE - Pt wire – Ag/AgCl, E(i) = -1.25 V (waiting time was 60 s), E(f) = 1.25 V vs. Ag/AgCl, with a scan rate of 1000 mV s^{-1}. Samples were purged of oxygen by bubbling nitrogen through the solutions for 5 min.

Quantitative HPLC analysis. The quantitative analyses of flupirtine maleate and D13223 were done with an Dionex HPLC system consisting of a P580 pump, an ASI-100 automated sample injector, a UVD170S UV/vis detector and a STH585 column oven. Analysis of the chromatograms was done with the CHROMELEON software package. For the analysis of flupirtine and D13223, a 250 * 4 mm Nucleosil 100-5 C18 AB column (Macherey-Nagel) preceded by a precolumn of the same material was used. The column was heated to 35 °C. Samples were diluted 1:1 into phosphate buffer and 100 µl of the sample were injected. Mobile phases were 30% acetonitrile/phosphate buffer (50 mM, pH 2.8) for flupirtine and 20% acetonitrile/phosphate buffer (50 mM, pH 2.8) for D13223. The flow rate was 0.7 ml/min. The retention times for flupirtine and D13223 were 6.67 ± 0.13 and 7.41 ± 0.30 min, respectively, with their respective eluents. Detection was done at λ = 345 and 344 nm for flupirtine and D13223, respectively. Peak height, which was more sensitive than peak area, was used to calculate of the percent decrease in the amount of substrate in the incubations. The molar concentrations were calculated with a calibration curve by using 5 external standards of either flupirtine or D13223.The relative precision of the analysis with microsomal incubations was < 1% for both flupirtine and D13223. The methods were linear ($r > 0.999$) between 10 and 23.3 µM for flupirtine and D13223.

HPLC/HRMS analysis. All chromatographic separations for HRMS measurements and the isolation of metabolites were done with an Agilent 1100 HPLC system consisted of a quaternary gradient pump, an autosampler and a solvent degasser. The column was connected

to the BNMI-HP unit for beam splitting (20:1) followed by the Bruker DAD UV-detector (Bruker Biospin, Rheinstetten, Germany) in parallel with the MicroTOF mass spectrometer (BRUKER Daltonics, Bremen, Germany). The MicroTOF mass spectrometer was equipped with an electrospray ion source (temperature 180 °C). Mass spectra were acquired with a scan range from 50 to 1500 m/z. All measurements were done in the positive mode. For all separations, a 125 * 4 mm LiChrospher 100 RP-18e (5 µm) column (Merck) proceeded by a precolumn of the same material was used. The flow rate was 0.5 ml/min. The chromatography was performed at 23 ± 2 °C. Detection was done at λ = 204, 247, and 319 nm (maxima of absorption) and 362 nm (minimum of absorption) for analytes. Metabolite fractions for MS/MS analysis with API 4000 mass spectrometer were collected manually. Eluents used in the gradients were acetonitrile (solvent B) and 50 mM ammonium acetate adjusted to pH 7.5 with 2.5% ammonia (solvent D). Solvent gradients for all chromatographic separations ran from 10 to 100% solvent B in 25 min, with the shapes of the gradients optimized for separations. These methods were used in the analysis of incubations of flupirtine or D13223 in the presence of microsomes with UDPGA, or in the presence of HRP and H_2O_2 with GSH

HPLC/MS/MS analysis. The MS/MS analysis of the two glucuronides of flupirtine and partly of metabolites from incubations of flupirtine with HRP were done in cooperation with Dr. Marcus Mickel from Applied Biosystems, (Applera Deutschland GmbH, Darmstadt, Germany). The equipment consisted of a Agilent gradient pump 1100, a column oven, an autosampler and a linear ion trap quadrupole mass spectrometer 3200 Q TRAP (AB Sciex Instruments). Source type was Turbo Spray with a source temperature of 450 °C. For all measurements the positive mode was used. A Phenomenex Synergi Hydro RP column, 150*2 mm (4 µm) was used for the chromatography with a flow rate of 0.3 ml/min. Separations were conducted using the following gradient: 95% A and 5% B for 30 s, followed by a linear increase to 100% B over 15.5 min, then followed by 2 min of 100% B. Afterwards column was reconstituted to the starting conditions over 7 min. Solvent A used in the gradient was 5 mM

ammonium acetate and, solvent B was methanol containing 5 mM ammonium acetate. The column was heated to 30 °C.

MS/MS analysis. The MS/MS analysis of all other metabolites of flupirtine and D13223, respectively, were done with an API 4000 mass spectrometer from Applied Biosystems (AB Sciex Instruments). Purified metabolite fractions were analyzed by flow injection analysis by using a solvent flow of acetonitrile/50 mM ammonium acetate buffer, pH = 7.5 (solvent ratios resulting from the further separations) at a flow rate of 10 and 20 µl/min, respectively. The mass spectrometer was equipped with an electrospray ion source (temperature 300 °C). CID-spectra (collision induced dissociation) were acquired for all metabolites with nitrogen as the collision gas. Collision energies used were in a range between 20 and 65 eV.

Stock solutions of substrates. Stock solutions of substrates were prepared as follows: 2.0 mM flupirtine maleate in water, 2.0 mM D13223 in 50 mM potassium phosphate buffer (pH 7.4) or 50 mM Tris-HCl (pH 7.4).

Spectral binding studies with rat liver microsomes. UV/vis spectra were recorded for both dexamethasone and phenobarbital induced rat liver microsomes (1.5 to 3 mg protein/ml), resuspended in 50% glycerol/phosphate buffer (50 mM, pH 7.4) with either ketoconazole (100 µM), cyclohexane (30 mM), flupirtine (100 and 400 µM) or D13223 (100 µM). Absorption spectra were recorded at room temperature with a single beam GENESYS 10UV spectrophotometer (Thermo Spectronic). Spectra without substrate were subtracted electronically from the spectra taken with substrate to give the difference spectra.

Incubations of flupirtine maleate and metabolite D13223 with rat liver microsomes and S9. Microsomes from non-induced as well as dexamethasone, rifampicin, phenobarbital, and ß-naphthoflavone induced rat livers were used. (Walter et al., 2003) The NADPH regenerating system and NADPH negative controls were incubated for 5 min at 37 °C in open tubes. Next, the required volume of the substrates was added, the solutions were mixed and divided into 2 ml reaction vials. The reactions were started by the addition of the microsomal suspension to

give a final concentration of 2 mg/ml protein (2 to 8 mg/ml protein for S9). The final volume of each incubation mixture was 1 ml containing 20 µM substrate, 0.5 mM $NADP^+$, 5 mM glucose-6-phosphate, 10 mM $MgCl_2*6H_2O$, 5 mM EDTA and 3.5 IU/ml glucose-6-phosphate dehydrogenase. Incubations were continued at 37 °C. At the appropriate times (0, 15, and 30 min) 180 µl were removed and added to 180 µl of ice cold acetonitrile. After mixing, the samples were placed on ice for 30 min to facilitate protein precipitation. Finally, the samples were centrifuged at 14,000 g at 0 °C for 10 min. The centrifuged samples were stored at -32 °C. Immediately prior to HPLC analysis the samples were mixed and centrifuged once more. The supernatant was analyzed by the Quantitative HPLC Analysis method (see above).

Incubations of flupirtine maleate and metabolite D13223 with human liver microsomes and S9. Incubations were done under the same conditions as described for rat liver microsomes. Modifications were: final protein concentration was 4 mg/ml for S9; final volume of each incubation mixture was 320 µl; sample volume 80 µl.

Incubations of flupirtine maleate and metabolite D13223 with MAO A and B. Substrates (20 µM) were incubated with recombinant human MAO A and B, respectively (6 IU/ml, determined by SIGMA-Aldrich for kynuramine deamination) in 50 mM potassium phosphate buffer (pH 7.4) at 37 °C for 60 min in a final volume of 280 µl. Control experiments were done with insect cell controls without the expressed enzymes. Samples were taken each 15 min and added to an equal volume of ice cold acetonitrile. After mixing, the samples were place on ice to facilitate protein precipitation. Finally, the samples were centrifuged at 14000 g at 0 °C for 10 min. The centrifuged samples were stored at -32 °C for a max. of 48 h before HPLC analysis. Immediately prior to HPLC analysis the samples were thawed, mixed and centrifuged once more at 14000 g at 0 °C for 10 min. The supernatant was analyzed by the Quantitative HPLC analysis method (see above).

Incubations of flupirtine maleate and metabolite D13223 with HRP and MPO. Incubations were done at 37 °C and contained the substrate (20 µM), desferoxamine (10 µM), and

peroxidase (0.05 to 0.3 IU/ml HRP, 1 to 3 IU/ml MPO) in 50 mM potassium phosphate buffer (pH 7.4). The reaction was initiated by addition of H_2O_2 (0.5 mM for flupirtine, 1.0 mM for D13223). Samples (100 µl) were taken at 0 and 10 min and treated with 150 IU catalase. The samples were incubated for additional 3 min, terminated by addition of 125 µl acetonitrile and placed on ice for 5 min. After centrifugation at 14,000 g and 0 °C for 10 min the samples were stored at -32 °C. The supernatant was analyzed by the Quantitative HPLC analysis method (see above).

Incubations of flupirtine maleate with porcine liver esterases and human *N*-acetyltransferases. All incubations were done at 37 °C in a 50 mM triethanolamine buffer (pH 7.5) containing 1 mM dithiothreitol, 1 mM ascorbic acid, 1 mM EDTA, 2 mg/ml porcine liver esterase 1 mM acetyl-CoA, an *N*-acetyl-CoA regenerating system (4.6 mM acetyl-*d,l*-carnitine and 3.75 U/ml of carnitine acetyl transferase) and 0.125 mg/ml human *N*-acetyltransferase (types 1 or 2). The reaction was started by adding a flupirtine maleate stock solution to give a final concentration of 40 µM. After 0, 15, 30, 45 and 60 min at 37 °C aliquots were removed and mixed 1:1 with ice cold acetonitrile and allowed to stand on ice for 15 min before being centrifuged for 5 min at 10,000 g at 0 °C. The supernatant (25 µl) was analyzed by the Quantitative HPLC Analysis method (see above) with an eluent of 20% acetonitrile/phosphate buffer (50 mM, pH 2.8) with detection at λ = 245 nm.

Incubations with HRP/MPO for HRMS. Peroxidase incubations (total volume 400 µl for HRP, 150 µl for MPO) were carried out at 37 °C and contained the substrate (20 or 150 µM), desferoxamine (10 µM), and enzyme (0.3 IU/ml HRP, 5 IU/ml MPO) in 50 mM Tris-HCl (pH 7.4). The reaction was initiated by addition of H_2O_2 (0.5 mM). Samples (100 µl/60 µl) were taken at 0, 10 and 30 (40) min and treated with 150 IU catalase. The samples were incubated for additional 3 min, reactions were terminated by addition of equivalent volume of acetonitrile. Samples were prepared and stored as described above for peroxidase incubations.

Incubations with HRP for structure determination of metabolites. Concentrations of substrate, enzyme and cofactors and incubation conditions were as described for HRMS experiment except the reaction was scaled up to 10 ml. After incubation for 30 min the mixture was incubated for additional 5 min with 1800 IU catalase. The reaction was terminated by addition of 5 ml acetonitrile and placed on ice for 10 min. After centrifugation at 8000 g and 0 °C for 10 min the mixture was removed completely from the pelleted protein and extracted with 5 ml of acetonitrile for three times. The collected organic phases were evaporated *in vacuo* and the aqueous phase was freeze dried. For HPLC analysis the residues were dissolved in 1 ml of acetonitrile and 1 ml of water, respectively.

For D13223, the incubations were done in a total volume of 750 µl. The incubation mixtures contained 150 µM D13223, 10 µM desferoxamine, and HRP (1 IU/ml) in 50 mM Tris-HCl (pH 7.4). The reaction was initiated by addition of 1 mM H_2O_2 and after 30 min another 20 µl H_2O_2 (11 mM stock solution) were added. After 60 min at 37 °C the mixture was incubated for 3 min with 1140 IU catalase. Then 470 µl acetonitrile was added and mixed, the samples were placed on ice for 10 min and centrifugated at 14000 g and 0 °C for 10 min. The supernatant was collected, the organic solvent removed *in vacuo* and the remaining aqueous phase was freeze dried. Samples were reconstituted for chromatography in 80 µl of water and 30 µl of acetonitrile.

Incubations with HRP and GSH for identification and structure determination of GSH-adducts. Incubations with HRP and GSH (total volume 750 µl) were carried out at 37 °C and contained the substrate (150 µM), desferoxamine (10 µM), GSH (1 mM) and HRP (0.3 IU/ml for flupirtine maleate or 1 IU/ml for D13223) in 50 mM Tris-HCl (pH 7.4). The reaction was initiated by addition of H_2O_2 (0.5 mM for flupirtine maleate or 1.0 mM for D13223). After 60 min, 1140 IU catalase were added for 3 min. To terminate the reaction acetonitrile was added and the samples were placed on ice for 30 min. After centrifugation at 14000 g at 0 °C for 10 min the supernatant was removed from the protein pellet and stored at -32 °C. The acetonitrile

phase was removed and the aqueous phase was extracted twice with 400 µl of acetonitrile followed by freeze-drying the aqueous phase. Lyophilized samples were reconstituted for chromatography in 100 µl of water.

For the analysis of the flupirtine metabolite with NMR the reaction was scaled up to a volume of 50 ml. From the centrifuged sample, the supernatant was removed and the acetonitrile evaporated *in vacuo*. The aqueous phase (12.5 ml) was drawn through a 6 ml Merck SPE column filled with 2 g of LiChrolut RP-18 (40-63 µm) that had been pre-conditioned with 20 ml acetonitrile and equilibrated with 20 ml water. The column was washed with 10 ml water and then the sample was eluted with 10 ml 30% acetonitrile/water. Remaining flupirtine was eluted with 50% acetonitrile/water. After freeze drying the sample was reconstituted in 75 µl 20% acetonitrile/10 mM ammonium acetate. The GSH-adduct was purified by preparative HPLC with a Phenomenex Synergi Polar RP column, 250*10.0 mm (4 µm) operated at room temperature. Injection volume was 25 µl. Chromatography was conducted with the following gradient: 90% A and 10% B linear increased to 40% B over 20 min, then followed by 2 min of 40% B and reconstitution to the starting conditions over 10 min. Solvent A used in the gradient was 10 mM ammonium acetate adjusted to pH 7.5 with 2.5% ammonia and solvent B was acetonitrile. With a flow rate of 2.3 ml/min the retention time for the adduct was 17.7 min. The eluent from collected fraction was removed by freeze drying.

NMR spectroscopy of GSH-adduct of flupirtine. All NMR spectra were obtained at 600.27 MHz at a nominal temperature of 298.5 K with a Bruker AVANCE-II 600 NMR spectrometer operated with TOPSPIN 2 software (both from Bruker Biospin GmbH, Rheinstetten, Germany). The GSH-adduct was dissolved in 0.5 ml D_2O in 5-mm NMR-glass tubes. The reference chemical shift was HDO at 4.80 ppm. For structure determination a ^1H and a two-dimensional $^1H,^1H$ correlation experiment (COSY) were done.

Incubations with human individual donor liver microsomes and glucuronic acid for HRMS and MS/MS. Microsomal glucuronidation of the substrate was studied by incubating 2 mg/ml microsomal protein in a final volume of 200 µl with 150 µM substrate and 5 mM UDPGA in the presence of 7 mM $MgCl_2$ in 100 mM Tris-HCl, pH 8.0. Samples were incubated at 37 °C for 2 h and the reaction was stopped by addition of an equivalent volume of ice-cold acetonitrile. After 30 min on ice, the samples were centrifugated at 14000 g and 0°C for 10 min. Samples were cooled to – 32 °C, the organic layer was removed and the aqueous phase was extracted twice with 125 µl of acetonitrile. After freeze drying of the aqueous phase, the lyophilized samples were reconstituted in 70 µl Tris-HCl (100mM, pH 8.0) for HPLC analysis. For the MS analysis of the glucuronide conjugates, the incubation volume was scaled up to 1 ml.

Results

Cyclic voltammetry studies

Figure 1 shows the cyclic voltammetry (CV) traces for flupirtine and D13223 at pH 7.4. The anodic and cathodic peak potentials ($E_{p,a}$ and $E_{p,c}$) for flupirtine were 0.535 V and 0.325 V, respectively (ΔE_p was 210 mV). The anodic and cathodic peak potentials for D13223 were 0.347 V and -0.271 V, respectively (ΔE_p was 618 mV). These data indicate that the D13223 is somewhat easier to oxidize than flupirtine while the reduction of oxidized D13223 is considerably more difficult than that of oxidized flupirtine.

FIGURE 1

The redox behavior for flupirtine and D13223 is not reversible, but the extent of irreversibility is considerably lower for flupirtine for the following reasons: 1) the ratio of peak cathodic and anodic currents (ip,c/ip,a) is not 1 as expected for reversible processes, 2) the difference in the peak potentials in not the expected 29.5 mV (for the two electron

reaction), 3) the smaller the rate of electron transfer, the larger the separation in peak potentials. (Bond, 1980)

Studies of NADPH-dependent metabolism in rat liver microsomes and S9 fraction

Metabolism of flupirtine and D13223 was investigated in incubations of 20 µM substrate with rat liver microsomes and S9-fraction. CYP-isoforms were induced in rat livers by treatment of the animals with specific inducing compounds, i.e., phenobarbital, ß-naphthoflavone, rifampicin and dexamethasone. (Correia, 1995) Control experiments with microsomes from untreated rats were also done.

Rifampicin and dexamethasone induced rat liver microsomes brought about some NADPH-dependent metabolism of both flupirtine and D13223. Substrate turnover of 8-18% for flupirtine and of 20-25% for D13223 was statistically significant. (data not shown). With all other microsomes the substrate turnover was less than 5%, comparable to the results from the control experiments without the cofactor NADPH.

With rat S9-fraction pooled from untreated rat livers 8-12% of flupirtine (incubations of 20 µM substrate) and 9-13% of D13223 were metabolized, respectively. This turnover was dependent on the cofactor NADPH and the protein content.

Spectral binding studies of flupirtine with rat liver CYP

Interactions between substrates and inhibitors of CYP can be studied by investigating the changes in the visible, “split Soret” absorption spectra caused by binding to the cytochrome (Jefcoate, 1978). Binding of a substrate to ferric CYP is characterized by a “type I” difference spectrum, whereby a shift in the intensity of the split Soret maximum at λ 390-405 nm at the expense of the absorption at λ 425-435 nm takes place. Binding of an inhibitor that can coordinate with the ferric iron causes a shift in intensity away from the maximum at λ 390-405 nm and towards the maximum at λ 425-435 nm (“type II” binding).

As expected the type I substrate cyclohexane and the type II inhibitor ketoconazole gave the typical difference spectra shown in Figure 2. On the other hand, neither flupirtine nor D13223 showed any signs of producing either type I or type II spectra in dexamethasone or phenobarbital induced rat liver microsomes (Figure 2), indicating that they only weakly interact with CYP. This is consistent with the turnover studies described above that both flupirtine and D13223 are only weak substrates for CYP.

FIGURE 2

NADPH-dependent metabolism in human liver microsomes and S9 fractions

For incubations with human liver microsomes samples from six individual donors and from one pool of 15 male and female donors (PH/GEO) were used. Because the studies with rat liver microsomes indicated that the rifampicin and dexamethasone inducible CYP-3A1 isoform most likely to be involved in flupirtine turnover, we focused our studies on the analogous enzyme in humans, CYP-3A4 (Correia, 1995; Guengerich, 1995). To estimate the CYP-3A4 activity in all human microsome preparations, the turnover of nifedipine to dehydronifedipine was determined. The K_m and V_{max} values for this reaction ranged from 18.3 to 23.4 µM and from 0.18 to 2.09 nmol/min/mg protein in the microsomal samples.

In all cases a flupirtine turnover of <5% was found with human microsomes containing NADPH (data not shown) regardless of the ability of the microsomes to metabolize nifedipine. With the metabolite D13223, incubations were done only with three individual samples and the pooled sample PH/GEO; nevertheless, a turnover of D13223 could not be detected either. In incubations of both flupirtine and D13223 with S9-liver fractions from four different human donors, substrate turnover of less than 7 % was observed (data not shown). No statistical significant differences in substrate decrease were found for incubations with and without NADPH.

Studies with monoamine oxidase.

Incubations of flupirtine and D13223 with recombinant human MAO A and B expressed in insect cells were carried out to investigate the ability of these enzymes to oxidatively metabolize the substances. With MAO A and B no detectable turnover of either substrate occurred, indicating that these enzymes do not participate appreciably in flupirtine metabolism in humans (data not shown).

Studies with peroxidases.

Peroxidases are known to oxidize some drugs and xenobiotics (O'Brian, 2000; Testa and Krämer, 2007) so we next studied the metabolism of flupirtine by human myeloperoxidase (MPO) and horse radish peroxidase (HRP). In contrast to CYP and MAO, both MPO and HRP were very capable of metabolizing flupirtine, whereby HRP was more efficient than MPO. With 0.05 IU/ml enzyme activity and 0.5 mM H_2O_2 a 35% turnover of flupirtine (starting concentration of flupirtine 20 µM) was found in 10 min. By raising the activity to 0.1 IU/ml HRP a 74% turnover of flupirtine occurred. In the case of MPO, activity was 3 IU/ml, which brought about a flupirtine turnover of 95% in 10 min.

In contrast to flupirtine, D13223 is a much poorer substrate for both peroxidases. With an enzyme activities of 0.1 IU/ml of HRP and 3 IU/ml of MPO only 15 and 9%, respectively, of D13223 (starting concentration also 20 µM) were metabolized in 10 min.

Characterization of flupirtine metabolites from incubations with peroxidases

HRP was used as a model enzyme to study the oxidative metabolism of flupirtine by peroxidases. In incubation mixtures containing 20 µM flupirtine and 0.3 IU/ml HRP or 3 IU/ml MPO only one product peak was detected with LC-HRMS with a retention time of ca. 6.8 min. The compound was found to have a m/z of 335, which was confirmed by LC-MS/MS experiments. The production scan showed a mean fragment ion at m/z = 303, suggesting loss

of O_2. Also some other fragment ions were observed with m/z-ratios decreased by 2 mass units compared to characteristic fragments of flupirtine (m/z 275; 257 for metabolite; m/z 277; 259 for flupirtine). The fragment ion at m/z = 318 in the MS/MS can be explained by a loss of OH from the proposed structure. This data leads us to propose that compound **4** could be a hydroperoxide of flupirtine, like the one shown in Scheme 2.

SCHEME 2

When the concentration of flupirtine was raised from 20 to 150 µM, smaller amounts of **4** were detected and most products appeared to be dimers and a trimer of flupirtine, which were more lipophilic then the parent compound and eluted later in the chromatogram than flupirtine. A representative chromatogram of such an incubation mixture is shown in Figure 3. Data from HRMS-measurements for metabolites **5** - **7** are given in Table 1. Qualitatively, the same products were detected when HRP was replaced with (by?) MPO, but the amounts of the products varied.

FIGURE 3,TABLE 1

After collecting the peaks corresponding to compounds **5-7** in Figure 3, MS/MS analyses were done to obtain structural information. Scheme 3 shows possible structures for compound **5,** which has a mass to charge ratio of 605**.** We favor the structure of the azo dimer; azo dimers have precedence in the HRP oxidation of benzidine (Josephy et al., 1983). The azo compound could be formed by coupling of two free radicals of flupirtine to give a hydrazine, followed by oxidation. Scheme 4 displays structures that are in accordance with the data for fragment ions observed in the mass spectra of compounds **6** and **7**. The formation of radical or quinoide intermediates is required for the coupling with another unchanged flupirtine to form the dimeric structures.

SCHEMES 3 and 4

It was considered that radical or quinoide intermediates might be trapped with GSH to form stable GSH conjugates. Incubations of flupirtine with HRP and H_2O_2 in the presence of 1 mM GSH

DMD Fast Forward. Published on December 12, 2008 as DOI: 10.1124/dmd.108.024364
This article has not been copyedited and formatted. The final version may differ from this version.

gave small amounts of a metabolite peak with a m/z of 610.209708 for $[M+H]^+$. The theoretical mass for a monoglutathione conjugate of flupirtine is 610.208986 for the quasimolecular ion $[M+H]^+$ with the molecular formular $C_{25}H_{33}FN_7O_8S$, which is in very good agreement with the experimental value. After separation of the compound by HPLC the substance was investigated directly by ESI-MS/MS (Figure 4). In the full scan mode the expected quasimolecular ion $[M+H]^+$ was detected at m/z = 610. Production scans (CID collision energy 30 eV) showed fragment ions resulting from neutral losses characteristic of GSH conjugates, namely the loss of Gly (m/z = 535; $[MH-75]^+$) and γ-Glu (m/z = 481; $[MH-129]^+$), which was also the base peak. Loss of glutathione residue gave the fragment ion at m/z = 305 as $[flupirtine+H]^+$. The appearance of an ion at m/z 337 indicates that all but the sulfur atom of glutathione has fragmented from the conjugate. The intense fragment at m/z = 231 likely represents loss of both glutathione and the carboethoxy groups. The weak fragment ion with m/z = 501, i.e. fragmentation of the fluorobenzylic side chain from the GSH-adduct, confirms that binding of the glutathione to the substrate takes place in the pyridine ring.

FIGURE 4

To determine the position of glutathione residue in the pyridine ring a 600 MHz ^{1}H-NMR-spectrum of the purified flupirtine GSH conjugate was recorded. With the data from the two-dimensional ^{1}H,^{1}H correlation experiment (COSY) all signals in the proton spectrum could be assigned. Proton chemical shifts for the GSH conjugate (**14**) are compared with those of flupirtine in Table 2. The H-5 of flupirtine (equivalent to position B in the adduct), a doublet at δ = 5.85 ppm, was missing in the spectrum of the GSH conjugate. Thus, the sulfur of glutathione binds at the C-5 (position B) of the pyridine ring of flupirtine.

TABLE 2

Identification of metabolites of D13223 from incubations with peroxidases

In incubations containing 20 µM of D13223, 1 IU/ml HRP and 1 mM H_2O_2 after 60 min only one metabolite (**11**) was observed by UV-detection. With the help of MS analysis, small

DMD Fast Forward. Published on December 12, 2008 as DOI: 10.1124/dmd.108.024364
This article has not been copyedited and formatted. The final version may differ from this version.

amounts of another, more polar metabolite (**10**) at 4.5 min were detected. This metabolite (**10**) was found in higher yields when the concentration of D13223 was raised to 150 µM. The chromatogram in Figure 5 also shows additional peaks in the incubation mixtures at the higher substrate concentration.

FIGURE 5

The low turnover rates of D13223 meant that the parent compound could still be seen in the chromatogram at 7.8 min. This was not the case with flupirtine, which by this time had completely disappeared under the same conditions.

For the metabolite **10** a molecular mass 273.113685 for $[M+H]^+$ was determined, which forms by a two-electron oxidation of D13223. The molecular formula of this compound should be $C_{14}H_{14}FN_4O$ with a theoretical mass of 273.114616. Possible structures of this compound are the two quinone diimines (**a**, **b**) and the imine (**c**), which as shown in Scheme 5 are tautomers of one other. Semi-empirical optimizations (both AM1 and PM3 with Gaussian 98) indicated the order of stability of the three tautomers to be: **c** > **b** > **a** (e.g., energies of -0.0226732, 0.0071204, 0.0639557 Hartrees, respectively, with PM3). The appearance of a fragment ion at m/z = 109 in the MS/MS spectrum indicates the loss of the fluorobenzyl chain, evidence for the presence of tautomers **a** and **b**. In the MS of the metabolite, some ions were observed with m/z-ratios decreased of 2 mass units compared to characteristic fragments of D13223 (m/z 231.177164 for metabolite; m/z 233.179166 for D13223).

SCHEME 5

For metabolite **11** with a molecular mass of 289.108952 for the $[M+H]^+$-quasimolecular ion the molecular formula $C_{14}H_{14}FN_4O_2$ (289.109530) was calculated. The [M + H+] of 289 m/z for the main metabolite **11** eluting at 8.9 min is consistent with the addition of oxygen to the quinone diimine of D13223. Two possible structures are shown in Scheme 6, however, not all data from the MS/MS are consistent with these proposals. NMR experiments are planned for further structure determination of this new metabolite.

SCHEME 6

Compounds **12** and **13** eluting at 11.5 and 15.3 min, respectively, are expected to be dimers of D13223 because of their m/z of 547 and 545, respectively. Because of the low yields of these products, further structure elucidation was not possible.

To trap potential reactive forms of D13223, GSH was added to the incubations with HRP and H_2O_2 as described for flupirtine. A metabolite peak with a molecular mass of 580.199554 for $[M+H]^+$ was found, which is consistent with the theoretical mass (580.198422) for a monoglutathione conjugate of D13223 ($[M+H]^+$) with the molecular formular $C_{24}H_{31}FN_7O_7S$. MS/MS and NMR analysis to confirm the adduct structure are still needed.

Studies on the esterase cleavage of flupirtine and the acetylation to D13223

To form D13223 from flupirtine, the carbamate group must be lost to yield descarboethoxyflupirtine, which could be acetylated by *N*-acetyltransferases (NAT). Carbamates are known to be cleaved either through CYP oxidation, as in the case of loratadine [Yumibe et al., 1996], or carboxylesterase hydrolysis, as in the cases of irinotecan and capecitabine [Humerickhouse et al., 2000; Quinney et al., 2005]. Since we observed very little CYP dependent oxidation with human microsomes, we focused our attention on reactions catalyzed by carboxylesterases. Thus, we incubated 40 µM flupirtine with porcine liver esterases either in the absence or presence of recombinant human NAT-1 and NAT-2 with acetyl-CoA and followed the reactions by HPLC. In both cases, a measurable loss of flupirtine was observed already at times less than 5 min. If no NAT/acetyl-CoA was present in the incubation, the formation of a hydrophilic product, presumably descarboethoxyflupirtine, was observed in the chromatogram that paralleled the loss of flupirtine. This product then disappeared itself with time to give way to a number of further unidentified, highly colored products. With the NAT/acetyl-CoA generating system present, none of these colored products were observed; instead a single peak with an identical retention time as D13223 at 7.3 min was

observed (Figure 6). The rates of formation of this metabolite were the same for either NAT-1 or NAT-2, indicating that descarboethoxyflupirtine is an equally efficient substrate for the both isoforms of NAT.

FIGURE 6

Identification of glucuronides of flupirtine and D13223 from incubations with human liver microsomes and UDPGA

When either flupirtine or D13223 were incubated with human liver microsomes and UDPGA, the formation of two glucuronides was observed. This was the case irrespective of the source of the individual donor microsomes (lots 1009, 1012 and 1022). Consistent with the formation of hydrophilic glucuronide metabolites, the HPLC retention times of the products are shorter compared to the parent compounds. The glucuronide with the shortest retention time also displays the smallest peak in the chromatograms for both substrates. Quantification of the glucuronides has not yet been possible due to the lack of material; due to the very low yields of the glucuronides, an isolation of pure products for use as standards for quantification with HPLC-UV- or MS-detection has not yet been possible. For all four glucuronides exact masses were determined and molecular formulars were calculated (Table 3).

TABLE 3

For the flupirtine metabolites (**15**) and (**16**) LC-MS/MS investigations were done with the entire incubation mixtures without enrichment or chromatographic procedures. Spectra of the glucuronides in each case show a fragment ion resulting from the neutral loss of glucuronic acid residue identical to $[flupirtine+H]^+$ (m/z = 305; $[MH-176]^+$). The flupirtine fragments at m/z 196 ($[flupirtineH - fluorobenzyl]^+$) and 109 (fluorobenzyl residue) were also observed. The product ion at m/z = 150 demonstrated a loss of ethanol from the fragment with m/z = 196. Two product ions at m/z 463 and 445 demonstrate the loss of one and two molecules H_2O, respectively, from the glucuronic acid residue (Figure 7).

FIGURE 7

Analogous to the two glucuronic acid metabolites of retigabine (Hempel et al. 1999), glucuronic acid residues would be expected to be bound at the primary (N2) and the secondary amino group (N6) of flupirtine (Scheme 7).

SCHEME 7

Conjugation with the carbamate nitrogen would not be expected because it is much less nucleophilic than either the nitrogen of the primary or the secondary amino group. From the MS/MS data a complete structural determination is not possible because no information on the position of the glucuronic acid residue has been obtained yet. Hempel and coworkers used NMR data from the retigabine glucuronide that formed most predominately to assign the positions of conjugation (Hempel et al.., 1999). Likewise, the assignment of the glucuronide isomers of flupirtine observed in the HPLC will require detailed NMR studies; this has been hampered thus far by the very small amounts of flupirtine glucuronides that can be isolated by HPLC.

Glucuronidation of D13223 was also studied under identical conditions as for flupirtine. For the MS/MS measurements of the glucuronides of D13223 (**19**) and (**20**), fractions eluting with the compounds were collected from the HPLC and analyzed by direct flow injection. In the full scan mode the quasimolecular ion $[M+H]^+$ at m/z 451 for both metabolites could be clearly detected. The production scan mode (CID) produced similar fragmentation patterns for both substances, the main differences were the relative intensities of the fragment ions (Figure 8).

FIGURE 8

The protonated ion of the unconjugated drug at m/z = 275 was found. The characteristic fragment ions of D13223 at m/z = 109 (known from flupirtine as the p-fluorobenzyl residue), m/z = 166 (monoacetylated triaminobenzene moiety after cleavage of the fluorobenzyl chain from D13223), m/z =179 (cleavage of the fluorophenyl residue from D13223) and m/z 232 and

233 (both for the loss of the acetyl group) were observed. As described for the glucuronides of flupirtine, the two fragment ions at m/z 433 and 415 indicate the loss of one or two molecules water from the glucuronic acid moiety. As already discussed for flupirtine, the position of glucuronide conjugation could not be established from MS data alone but can only be implied from the analogous data from retigabine.

Discussion

Antioxidative properties have been ascribed to flupirtine (Gassen et al. 1998); indeed, these properties may play a role in some of the neuroprotective activity of the drug (Boscia et al., 2006). Thus, it is reasonable to assume that flupirtine will be oxidized under biological conditions. Based on the anodic potentials in the CV studies, both flupirtine and D13223 are favored to undergo oxidations under physiological conditions. Furthermore, our CV studies show that flupirtine undergoes less irreversible redox reactions than D13223. The observation that the redox reactions for flupirtine and D13223 are irreversible indicates that the oxidation products of both compounds are reactive species. This was substantiated later by the observation of dimer and polymer formation during the peroxidase catalyzed oxidation of flupirtine.

Three oxidative enzyme systems were studied for their ability to metabolize flupirtine: 1) the CYP system, 2) the MAO A and B flavin-dependent enzymes, and 3) peroxidases. The role of CYP in the metabolism of flupirtine was investigated first.

When flupirtine and D13223 were incubated in the presence of induced and non-induced rat liver microsomes, some NDAPH-dependent turnover of flupirtine and D13223 by liver microsomes was observed with rats pretreated with rifampicin or dexamethasone (i.e., induction of CYP-3A1). This indicates that the CYP-3A1 isozyme participates to some extent in the metabolism of flupirtine and D13223 in rats. Likewise, with S9 fractions from livers of

untreated rats, small but statistically significant decreases in both flupirtine and D13223 were found that were NADPH dependent. However, the interactions of flupirtine and D13223 with rat liver CYP are very weak, as evidenced by the failure of both to produce CYP difference spectra, either of the type I or type II variety, in microsomal preparations.

In comparable studies with pooled liver microsomes from 15 human donor and 6 microsomal samples from individual donors (both male and female), no significant turnover of either flupirtine or D13223 was observed over 30 min., even though several of these microsomal preparations where shown to have strong CYP-3A4 activity (quantified by nifedipine oxidation). Thus, flupirtine and D13223 do not appear to be substrates for the human CYP system at therapeutic concentrations. These data are in keeping with those reported by McNeilly and coworkers for retigabine (**3**) (McNeilly et al., 1997); they concluded that oxidative metabolism of **3** was minimal in preparations of human liver microsomes and liver slices supplemented with NADPH.

Monoamine oxidases generally convert primary amines to imines, leading to the hydrolytic cleavage of the C=N bond to yield an aldehyde. Some secondary amines are also known to be oxidatively metabolized, resulting in the formation of the partly or completely dealkylated amine and metabolites with aldehyde groups (Kalgutkar et al., 2001). As discussed above, oxidative cleavage of the p-fluorobenzyl chain is suspected in the pathway to the known metabolite 4-fluorohippuric acid, and cleavage by MAO to form p-fluorobenzaldehyde as an intermediate was postulated. However, in incubations of either flupirtine or D13223 with human recombinant MAO A and B, neither substrate was metabolized. Thus, MAO isozymes appear unlikely to participate in the *in vivo* metabolism of flupirtine.

On the other hand, both flupirtine and D13223 are excellent substrates for the peroxidase enzymes HRP and MPO. Turnover of flupirtine to oxidized products is very rapid and complete when incubated with either HRP or MPO in the presence of hydrogen peroxide. Hydrogen peroxide alone had no influence on the stability of flupirtine.

Incubations of flupirtine with HRP resulted in dimeric metabolites, which were characterized by LC-HRMS and MS/MS methods. Formation of dimers and oligomers could occur through one or two electron oxidations. Radicals and quinoide structures have been described as intermediates of peroxidase oxidations for a variety of aromatic amines (Josephy et al., 1983; Eling et al., 1990). However, under *in vivo* conditions, the formation of flupirtine dimers is not expected because of low plasma concentrations of the drug [C_{max} ca. 6 µM in humans (Hlavica and Niebch, 1985)] compared to the *in vitro* experiments reported here. Reactions between oxidized flupirtine and GSH would appear more likely.

When 1 mM GSH was included to the incubations, very low flupirtine turnover was observed. Because of the higher concentration of GSH in the incubations relative to flupirtine, rapid oxidation of GSH to GSSG with hydrogen peroxide can also take place, so that the rate of flupirtine oxidation and coupling with GSH is greatly reduced. Alternatively, the low yields of GSH conjugates of flupirtine could also be due to the involvement of GSH in the reduction of oxidized flupirtine species back to flupirtine before dimers/trimers can form; i.e. GSH acts as an antioxidant. To confirm which of these two hypotheses is operative will require further investigations.

Nevertheless, formation of GSH conjugates was observed in incubations of flupirtine with HRP/H_2O_2 after addition of GSH. One GSH conjugate of flupirtine was isolated and characterized by MS and NMR. Thus, enzymatic oxidation of flupitine leads to intermediates that can be trapped with GSH. Based on the prediction from these *in vitro* studies, we have recently isolated and characterized a mercapturic acid metabolite of flupirtine from the urine of human volunteers after oral ingestion of the drug. The *N*-acetylcysteine residue is bound to the pyridine ring of flupirtine at the same position as the glutathione side chain of the GSH adduct formed *in vitro*. These results illustrate the importance of studying GSH-adduct formation *in vitro* to help predict *in vivo* metabolism of a drug.

Our findings that glutathione adducts of flupirtine can form *in vitro* helps explain earlier observations that when radioactive flupirtine was administered to rats, hydrophilic metabolites of flupirtine were observed in rat bile that could not be cleaved back to flupiritine by sulfatase or ß-glucuronidase. (Hlavica and Niebch, 1985) Our data implicate glutathione conjugates as these biliary metabolites but further work will be needed to confirm this.

D13223 is a poorer substrate for peroxidases than flupirtine, which may be because D13223 is considerably more hydrophilic than flupirtine. Interestingly, D13223 preferentially forms an oxidation product containing one more oxygen atom per molecule. Consistent with the CV data that oxidized D13223 is more difficult to reduce than oxidized flupirtine, a relatively stable quinone diimine was also observed in the incubations with D13223, while dimers were formed only in very low yields. No such quinone diimine was observed for flupirtine under the same conditions. This may also be due to the extreme reactivity of the flupirtine diimine, which dimerize and trimerize more rapidly than D13223. Like with flupirtine, a GSH adduct was observed by LC-HRMS when GSH was added to the incubations of D13223 with HRP.

A further phase I pathway that we considered was the hydrolysis of the carbamate group, which can be catalyzed by carboxylesterases. (Humerickhouse et al., 2000; Quinney et al., 2005) Carboxylestersase are widely distributed in the body: blood serum, leukocytes, hepatocytes and cells of the intestine have high activities. Flupirtine and D13223 are both stable in fetal calf serum (data not shown), thus esterases in blood serum do not appear to be involved in metabolism. We observed, however, that porcine liver esterases are efficient at metabolizing flupirtine, presumably by hydrolyzing the carbamate group. Furthermore, when an acetyl-CoA regenerating system is present with either NAT-1 or NAT-2, the presumptive product of that hydrolysis, descarboethoxyflupirtine, is efficiently acetylated to D13223 *in vitro*. Although it was not possible to determine the enzyme kinetic parameters K_m and V_{max} values for the acetylation reaction because descarboethoxyflupirtine is too instable in aqueous

solution, from the rate of D13223 formation under identical conditions both isoforms of NAT appear to be equally efficient in catalyzing *N*-acetylation of descarboethoxyflupirtine.

N-Glucuronide conjugates have been reported previously for retigabine (McNeilly et al., 1997; Hiller et al., 1999; Borlak et al., 2006) as well as a variety of aromatic amines (Chiu and Huskey, 1998; Green and Tephly, 1996; Green and Tephly, 1998; Green et al. 1998; Zenser et al. 1996), but until now there were no published data on glucuronide formation with flupirtine. In incubations of flupirtine and the metabolite D13223 with human liver microsomes and the co-substrate UDPGA, in both case the formation of two glucuronides was observed with LC-MS/MS methods. However, the very low yields of these conjugates made it impossible to obtain quantitative data on possible interindividual variability of glucuronidation rates. Early studies on flupirtine metabolism excluded the formation of such metabolites based on enzyme cleavage studies (Obermeier et al. 1985; Hlavica and Niebch, 1985). However, this evidence indicates that flupirtine, like retigabine, is susceptible to *N*-glucuronidation albeit to a lesser extent. During the preparation of this manuscript we were made aware of a confidential AWD study report by H. Schupke and A. Gasparic from 1996 comparing the glucuronidation of flupirtine with retigabine in human liver microsomes. They found the formation of two glucuronides in both cases, with retigabine conjugation was >10-fold more efficient than with flupirtine. However, they did not characterize the glucuronides of flupirtine by MS as we have done.

Scheme 7 summarizes the findings of our *in vitro* metabolism studies. CYP and MAO do not appear to play an appreciable roll in the oxidative metabolism of flupirtine. On the other hand, this work shows for the first time that flupirtine is readily oxidized by peroxidases, such as human MPO. The products of peroxidase oxidation are likely to be quinone diimines (e.g., **10**), which at higher concentrations can dimerize and trimerize. More relevant for drug metabolism are reactions with bionucleophiles, such as GSH, that can undergo addition reactions to the oxidized products; indeed a GSH conjugate of flupirtine (**14**) was detected in

incubations with HRP. Thus, this work predicts the presence of mercapturic acid metabolites in urine of patients taking flupirtine. A further phase I reaction that is reported here for the first time is the hydrolysis of the carbamate group of flupirtine by liver carboxylesterases. Moreover, the putative descarboethoxy product, which is particularly sensitive to oxidation, is efficiently acetylated to D13223 by human NAT-1 and NAT-2. This is a significant finding that both isozymes are equally effective in producing D13223 *in vitro*. Thus, NAT polymorphism may not be important in the *in vivo* metabolism of flupirtine because both isozymes are equally efficient at acetylation. Another conjugation reaction that we predict here for flupirtine is with glucuronic acid; two isomeric *N*-glucuronides were identified in microsomal incubations of both flupirtine (**15** and **16**) and D13223 (**19** and **20**) with UDP-glucuronic acid.

SCHEME 7

Nevertheless, we were unable to clarify the metabolic pathway that leads to the cleavage of 4-fluorobenzaldehyde, the putative source of 4-fluorohippuric acid, which comprising ca. 20% of the excreted dose of flupirtine in humans (Hlavica and Niebch, 1985). 4-Fluorobenzaldehyde could form by hydrolysis of an imine of flupirtine or D13223, which could theoretically form if the quinone diimine tautomerized, as shown with D13223 in Scheme 5. However, we not yet observed 4-fluorobenzaldehyde directly in the incubations of HRP with either flupirtine or D13223, which may be due to the instability of the aldehyde under the incubation conditions. Ongoing work is aiming to clarify this pathway.

In conclusion, these *in vitro* studies have been useful in identifying potential new metabolites of flupirtine (e.g., mercapturic and glucuronic acid conjugates) as well as in judging the importance of polymorphism in the formation of the acetylated metabolite D13223.

This information will be useful in planning and interpreting future clinical pharmacokinetic studies.

Acknowledgements

We thank Simon Müller for technical assistance in the MS investigations and Dr. Markus Mickel of Applied Biosystems for performing the LC-MS/MS analyses of the flupirtine glucuronides.

References

Bond AM (1980) In: Modern Polarographic Methods in Analytical Chemistry, Marcel Dekker, New York, p. 187.

Borlak J, Gasparic A, Locher M, Schupke H, Hermann R (2006) N-Glucuronidation of the antiepileptic drug retigabine: Results from studies with human volunteers, heterologously expressed human UGTs. human liver, kidney, and liver microsomal membranes of Crigler-Najjar type II Metabolism. *Clin. Exper*. **55:**711-721.

Boscia F, Annunziato L, Taglialatela M (2006) Retigabine and flupirtine exert neuroprotective actions in organotypic hippocampal cultures. *Neuropharmacol*. **51**:283-294.

Chiu SHL, Huskey SEW (1998) Species differences in *N*-glucuronidation. *Drug Metab. Dispos*. **26:**838-847.

Correia MA (1995) Rat and human liver cytochromes P450, in *Cytochrome P450* (Ortiz de Montellano, PR ed) pp 607-630, Plenum Press, New York.

Darius H, Schrör K (1985) The action of flupirtine on prostaglandin formation and platelet aggregation in vitro. Arzneim-Forsch. (Drug Res.) **35**: 55-59.

Eling TE, Thompson DC Foureman GL, Curtis JF, and Hughes MF (1990) Prostaglandin H synthase and xenobiotic oxidation. *Annu. Rev. Pharmacol. Toxicol.* **30:**1-45.

Gassen M., Pergande G, Youdim MBH (1998) Antioxidant properties of the triaminopyridine, flupirtine. *Biochem Pharmacol*. **56**:1323-1329.

Green MD, Tephly TR (1996) Glucuronidation of amines and hydroxylated xenobiotics and endobiotics catalyzed by expressed human UGT1.4 protein. *Drug Metab. Dispos.* **24:**356-63.

Green MD, King CD, Mojarrabi B, Mackenzie PI, Tephly TR (1998) Glucuronidation of amines and other xenobiotics catalyzed by expressed human UDP-glucuronosyltransferase 1A3. *Drug Metab. Dispos*. **26:**507-512.

Green MD, Tephly TR (1998) Glucuronidation of amine substrates by purified and expressed UDP-glucuronosyl transferase proteins. *Drug Metab. Dispos.* **26:**860-867.

Guengerich, FP (1995) Human cytochrome P450 enzymes, in *Cytochrome P450* (Ortiz de Montellano, PR ed) pp 473-535, Plenum Press, New York.

Hempel R, Schupke H, McNeilly PJ, Heinecke K, Kronbach C, Grunwald C, Zimmermann G, Griesinger C, Engel J, Kronbach T (1999) Metabolism of retigabine (D-23129). A novel anticonvulsant. *Drug Metab. Dispos.* **27:**613-622.

Hiller A, Nguyen N, Strassburg CP, Li Q, Jainta H, Pechstein B, Ruus P, Engel J, Tukey RH, Kronbach T (1999) Retigabine N-glucuronidation and its potential role in enterohepatic circulation. *Drug Metab. Dispos.* **27:**605-612.

Hlavica P, Niebch G (1985) Untersuchungen zur Pharmakokinetik und Biotransformation des Analgetikums Flupirtin beim Menschen. *Arzneim.-Forsch. (Drug Res.)* **35**:67-74

Humerickhouse R, Lohrbach K, Li L, Bosron WF, Dolan ME (2000) Characterization of CPT-11 hydrolysis by human liver carboxylesterase isoforms hCE-1 and hCE-2. *Cancer Res.* **60**:1189-1192.

Jakob R, Krieglstein J (1997) Influence of flupirtine on a G-protein coupled inwardly rectifying potassium current in hippocampal neurons. *Brit. J. Pharmacol.* **122**:1333-1338.

Jakovlev V, Sofia RD, Achterrrath-Tuckermann U, von Schlichtegroll A, Thiemer K (1985) Untersuchungen zur pharmakologischen Wirkung von Flupirtin einem strukturell neuartigen Analgetikum. *Arzneim.-Forsch. (Drug Res.)* **35**:30-43.

Jefcoate CR (1978) Measurement of substrate and inhibitor binding to microsomal cytochrome P-450 by optical-difference spectroscopy. *Methods Enzymol*. **52**:258-279.

Josephy PD, Eling TE, Mason RP (1983) Cooxidation of benzidine by prostaglandin synthase and comparison with the action of horseradish peroxidase. *J. Biol. Chem.* **258:**5561-5569.

Kalgutkar AS, Dalvie DK, Castagnoli N, Taylor TJ (2001) Interactions of nitrogen-containing xenobiotics with monoamine oxidase (MAO) isozymes A and B: SAR studies on MAO substrates and inhibitors. *Chem. Res. Toxicol.* **14**:1139-1162.

Kornhuber J, Maler M, Wiltfang J, Bleich S, Degner D, Ruther E (1999a) Opening of neuronal K^+ channels by flupirtine. *Fortschritt. Neurol. Psych.* **67**:466-475.

Kornhuber J, Bleich S, Wiltfang, J,Maler M, Parsons CG (1999b) Flupirtine shows functional NMDA receptor antagonism by enhance Mg^{2+} block via activation of voltage independent potassium channels. *J Neur. Trans.* **106**:857-867.

McNeilly PJ, Torchin CD, Anderson LW, Kapetanovic IM, Kupferberg HJ, Strong JM (1997) In vitro glucuronidation of D-23129, a new anticonvulsant by human liver microsomes and liver slices. *Xenobiotica* **27**:431-441.

Obermeier K, Niebch G, Thiemer K (1985) Untersuchungen zur Pharmakokinetik und Biotransformation des Analgetikums Flupirtin bei Ratte und Hund. *Arneim.-Forsch. (Drug Res.)* **35**:60-67.

O'Brian PJ (2000) Peroxidase. *Chem.-Biol. Interact.* **129**:113-139.

Otto M, Cepek L, Ratzka P, Doehlinger S, Boekhoff I, Wiltfang J, Irle E, Pergande G, Ellers-Lenz B, Windl O, Kretzschmar HA, Poser S, Prange H. (2004) Efficacy of flupirtine on cognitive function in patients with CJD. *Neurology* **62**:714-718.

Pierce RH, Franklin CC, Campbell JS, Tonge RP, Chen W, Fausto N, Nelson SD, Bruschi SA (2002) Cell culture model for acetaminophen-induced hepatocyte death in vivo. *Biochem. Pharmacol*. **64**:413-424.

Quinney SK, Sanghani SP, Davis WI, Hurley TD, Sun Z, Murry DJ, Bosron WF (2005) Hydrolysis of capecitabine to 5'-deoxy-5-fluorocytidine by human carboxylesterases and inhibition by loperamide. *J. Pharmcol. Exper. Therap.* **313**:1011-1016.

Rostock A, Tober C, Rundfeldt C, Bartsch R, Engel J, Polymeropoulos E, Kutscher B, Löscher W, Hönack D, White H, Wolf H (1996) D23129: A new anticonvulsant with a broad spectrum activity in animal models of epileptic seizures. *Epilepsy Res.* **23:**211-223.

Schröder HC, Müller WEG (2002) Neuroprotective effect of flupirtine in prion disease. *Drugs* **49**:49-58.

Schuster G, Schwarz M, Block F, Pergande G, Schmidt WJ (1998) Flupirtine: A review of its neuroprotective and behavioural properties. *CNS Drug Rev.* **4**:149-164.

Seydel JK, Schaper KJ, Coats EA, Cordes HP, Emig P, Engel J, Kutscher B, Polymeropoulos EE (1994) Synthesis and quantitative structure-activity relationships of anticonvulsant 2,3,6-triaminopyridines. *J. Med. Chem.* **37**: 3016-3022.

Stoll AL (2000) Fibromyalgia symptoms relieved by flupirtine: an open-label case series. *Psychosomatics*. **41**:371-372.

Szelenyi I, Nickel B (1991) Pharmacological profile of flupirtine, a novel centrally acting. non-opioid analgesic drug. *Agents Actions Suppl.* **32**:119-23

Testa B, Krämer SD (2007) The biochemistry of drug metabolism- an introduction. *Chem. Biodiv.* **4**:257-405.

Thompson DC, Eling TE (1991) Reactive intermediates formed during the peroxidative oxidation of anisidine isomers. *Chem. Res. Toxicol.* **4:**474-81.

Walter R, Ullmann C, Thümmler D, Siegmund W (2003) Influence of propiverine on hepatic microsomal cytochrome P450 enzymes in male rats. *Drug Metab. Dispos.* **31**:714-717.

Yumibe N, Huie K, Chen KJ, Snow M, Clement RP, Cayen MN (1996) Identification of human liver cytochrome P450 enzymes that metabolize the nonsedating antihistamine loratadine - Formation of descarboethoxyloratadine by CYP3A4 and CYP2D6. *Biochem. Pharmacol.* **51**:165-172.

Zenser TV, Lakshmi VM, Davis BB (1998) N-Glucuronidation of benzidine and its metabolites; role in bladder cancer. *Drug Metab. Dispos.* **26:**856-859.

Footnotes

This work was supported by AWD.pharma GmbH & Co. KG. OV gratefully acknowledges the support (Grant 1QS500040581) from the Academy of Sciences of the Czech Republic.

Figure Captions

Figure 1. Cyclic voltammograms of D13223 (above) and flupirtine (below), dissolved in Tris-buffer (0.1 M, pH 7.4) both at concentrations of 1.0 mM.

Figure. 2. Difference spectra obtained from incubations of flupirtine (100 or 400 µM), D13223 (100 µM), ketoconazole (100 µM) and cyclohexane (30 mM) with either dexamethasone (upper figure) or phenobarbital (lower figure) induced rat liver microsomes.

Figure 3. Representative chromatogram of an incubation of 150 µM flupirtine with 0.3 IU/ml HRP and 0.5 mM hydrogen peroxide after an incubation time of 30 min. Molecular masses of the $[M+H]^+$-ions of the compounds are shown.

Figure 4. ESI/MS/MS-spectrum of flupirtine GSH-adduct **14.**

Figure 5. Representative chromatogram from incubation mixtures of 150 µM D13223 with HRP. Molecular masses of the $[M+H]^+$-ions of the compounds are shown.

Figure 6. Representative HPLC chromatograms obtained from the reactions of 40 µM flupirtine with porcine liver esterase, acetyl-CoA regenerating system and human recombinant NAT1 (upper figure) or NAT2 (below) at 37 °C. Chromatograms were obtained after 0, 15, 30, 45 and 60 min of incubation. D13223 and flupirtine have retention times of 7.3 and 21.3 min, respectively.

Figure 7. MS/MS-spectra of the flupirtine glucuronides **15** and **16**. The assignment of the structures to the spectra is arbitrary because the isomers can not be distinguished by MS.

Figure 8. MS/MS-spectra of D13223glucuronides **19** and **20**. The assignment of the structures to the spectra is arbitrary because the isomers can not be distinguished by MS.

DMD Fast Forward. Published on December 12, 2008 as DOI: 10.1124/dmd.108.024364
This article has not been copyedited and formatted. The final version may differ from this version.

Table 1. Data from HRMS-measurements of metabolites from incubations of 150 µM flupirtine maleate with HRP and H_2O_2

Metabolite	Retention time in min	$[M+H]^+$ (HRMS)	Theoretical mass $[M+H]^+$	Calculated molecular formula
5	13.8	605.243174	605.243084	$C_{30}H_{31}F_2N_8O_4$
6	14.7	607.258937	607.258734	$C_{30}H_{33}F_2N_8O_4$
7	15.1	607.259010		

DMD Fast Forward. Published on December 12, 2008 as DOI: 10.1124/dmd.108.024364
This article has not been copyedited and formatted. The final version may differ from this version.

Table 2. 600 MHz ^{1}H-NMR (D_2O) for the GSH conjugate **14** and flupirtine (in parentheses)

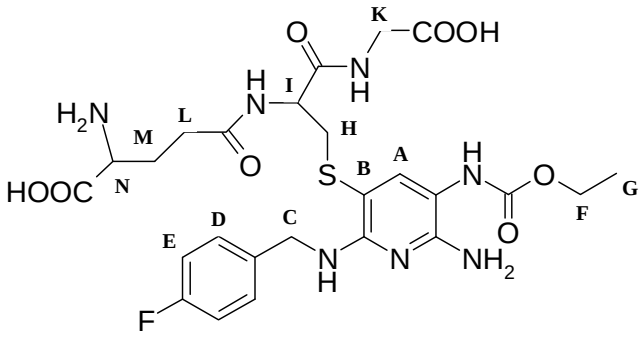

proton	^{1}H δ[ppm]	Intensity	Multiplicity	Coupling constants J [Hz]
A	7.43 (7.48)	1 (1)	s (d)	(8.9 to B)
D	7.43 (7.43)	2 (2)	m (dd)	(5.5 to Fluor; 8.6 to E)
E	7.14 (7.19)	2 (2)	t (t)	8.9 to Fluor/D (8.9 to Fluor/D)
B	(6.03)	(1)	(d)	(8.9 to A)
C	4.59 (4.55)	2 (2)	dd (s)	^{2}J 15.2 to C
I	4.43	1	dd	4.3 to H_B 8.6 to H_A
F	4.20 (4.22)	2 (2)	q (q)	6.7 to G (6.7)
K, N	3.75	3	m	
H_B	3.16	1	dd	^{2}J 14.4 to H_A 4.3 to I
H_A	2.97	1	dd	^{2}J 14.4 to H_B 8.6 to I
L	2.49	2	m	
M	2.14	2	m	
G	1.33 (1.32)	3 (3)	t (t)	6.7 to F (6.7)

DMD Fast Forward. Published on December 12, 2008 as DOI: 10.1124/dmd.108.024364
This article has not been copyedited and formatted. The final version may differ from this version.

Table 3. Data from HRMS-measurements of glucuronides from incubations of 200 µM flupirtine (**15**, **16**) and D13223 (**19**, **20**) with human liver microsomes and UDPGA

Metabolite	Retention time in min	$[M+H]^+$ (HRMS)	Theoretical mass $[M+H]^+$	Calculated molecular formula
15	7.2	481.172827	481.172918	$C_{21}H_{26}FN_4O_8$
16	8.1	481.172990		
19	8.1	451.162356	451.162354	$C_{20}H_{24}FN_4O_7$
20	10.2	451.161873		

DMD Fast Forward. Published on December 12, 2008 as DOI: 10.1124/dmd.108.024364
This article has not been copyedited and formatted. The final version may differ from this version.

Scheme 1. Structures of flupirtine, D13223 and retigabine

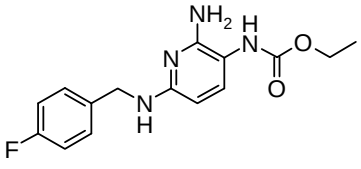

flupirtine (**1**)

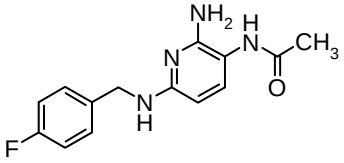

D13223 (**2**)

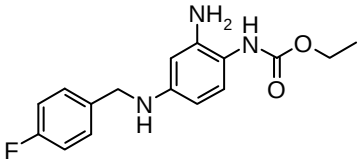

retigabine (**3**)

DMD Fast Forward. Published on December 12, 2008 as DOI: 10.1124/dmd.108.024364
This article has not been copyedited and formatted. The final version may differ from this version.

Scheme 2: Possible structure of metabolite **4**

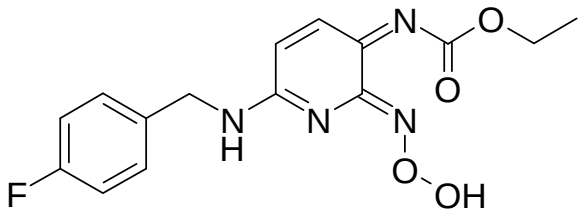

DMD Fast Forward. Published on December 12, 2008 as DOI: 10.1124/dmd.108.024364
This article has not been copyedited and formatted. The final version may differ from this version.

Scheme 3 : Possible structures for metabolite **5**

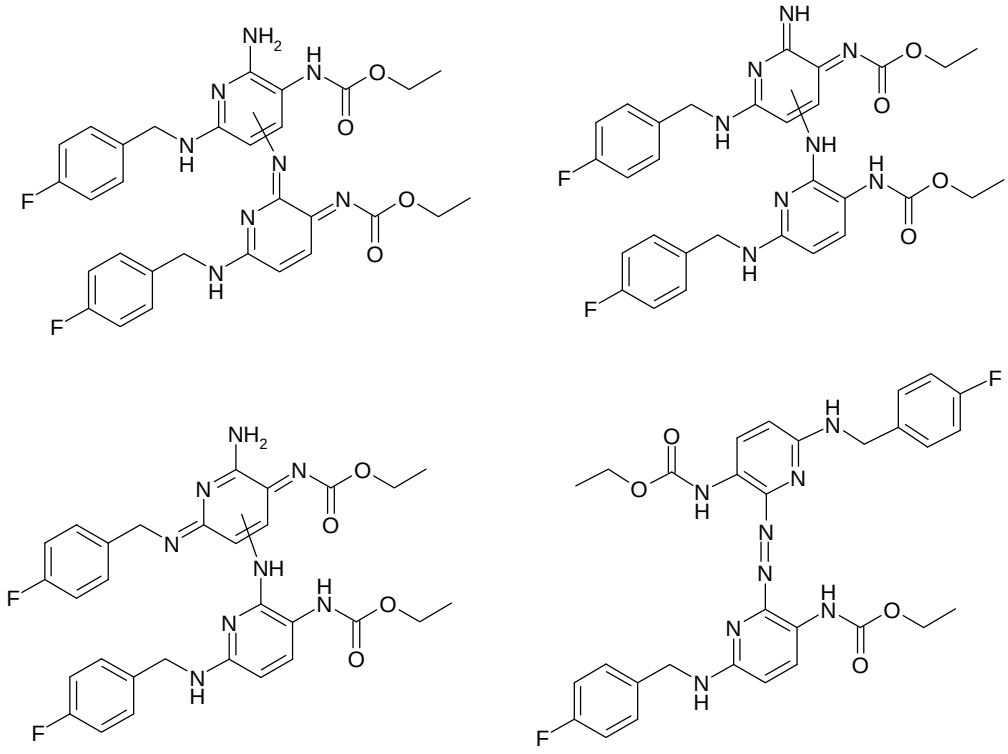

Scheme 4: Proposed structures of the metabolites **6** and **7**

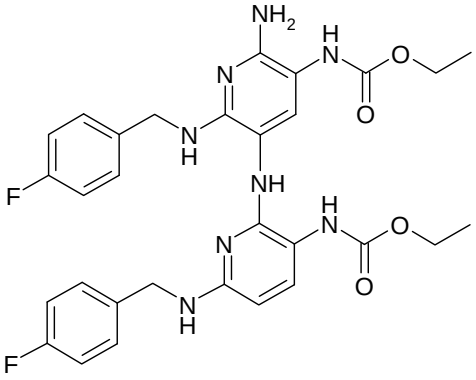

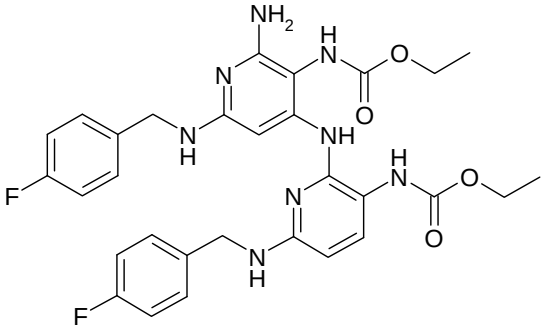

DMD Fast Forward. Published on December 12, 2008 as DOI: 10.1124/dmd.108.024364
This article has not been copyedited and formatted. The final version may differ from this version.

Scheme 5: Proposed structures of metabolite **10** from incubations of D13223 with HRP

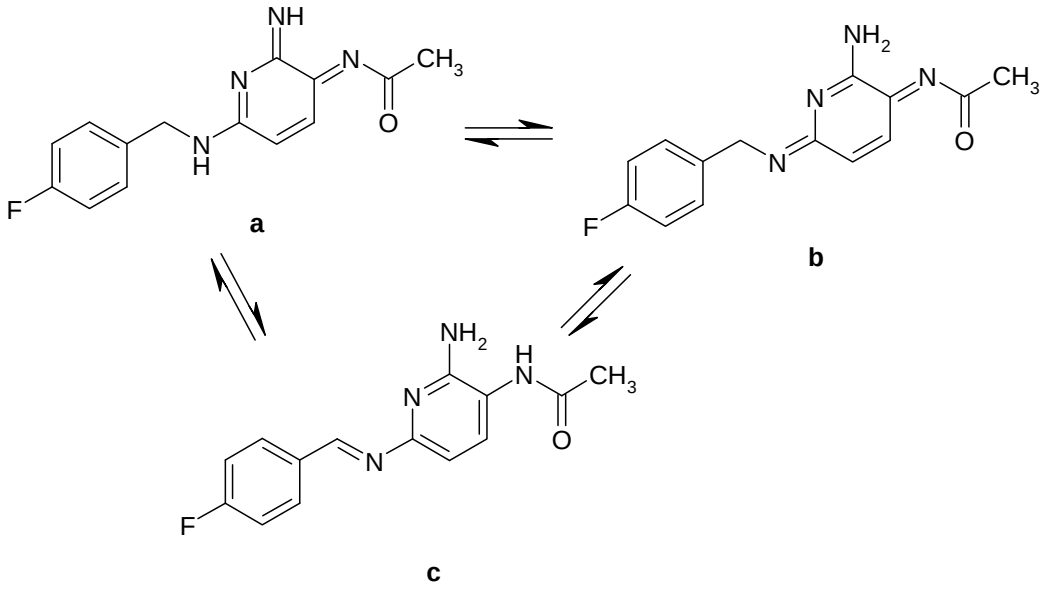

DMD Fast Forward. Published on December 12, 2008 as DOI: 10.1124/dmd.108.024364
This article has not been copyedited and formatted. The final version may differ from this version.

Scheme 6: Structures of metabolite **11** consistent with the determined molecular formula

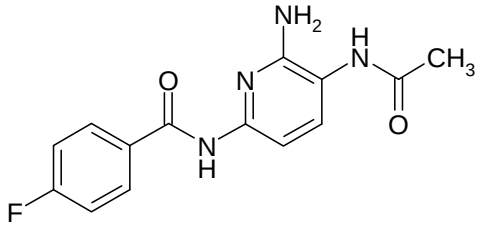

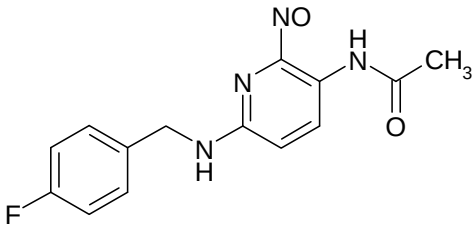

DMD Fast Forward. Published on December 12, 2008 as DOI: 10.1124/dmd.108.024364
This article has not been copyedited and formatted. The final version may differ from this version.

Scheme 7: Proposed *in vitro* metabolic pathways of flupirtine. Compounds in brackets were not isolated and/or characterized. The assignment of the structures to the pairs of glucuronides 15/16 and 19/20 is arbitrary (see text). The pathway leading to the formation of 4-fluorohippuric acid is not yet known.

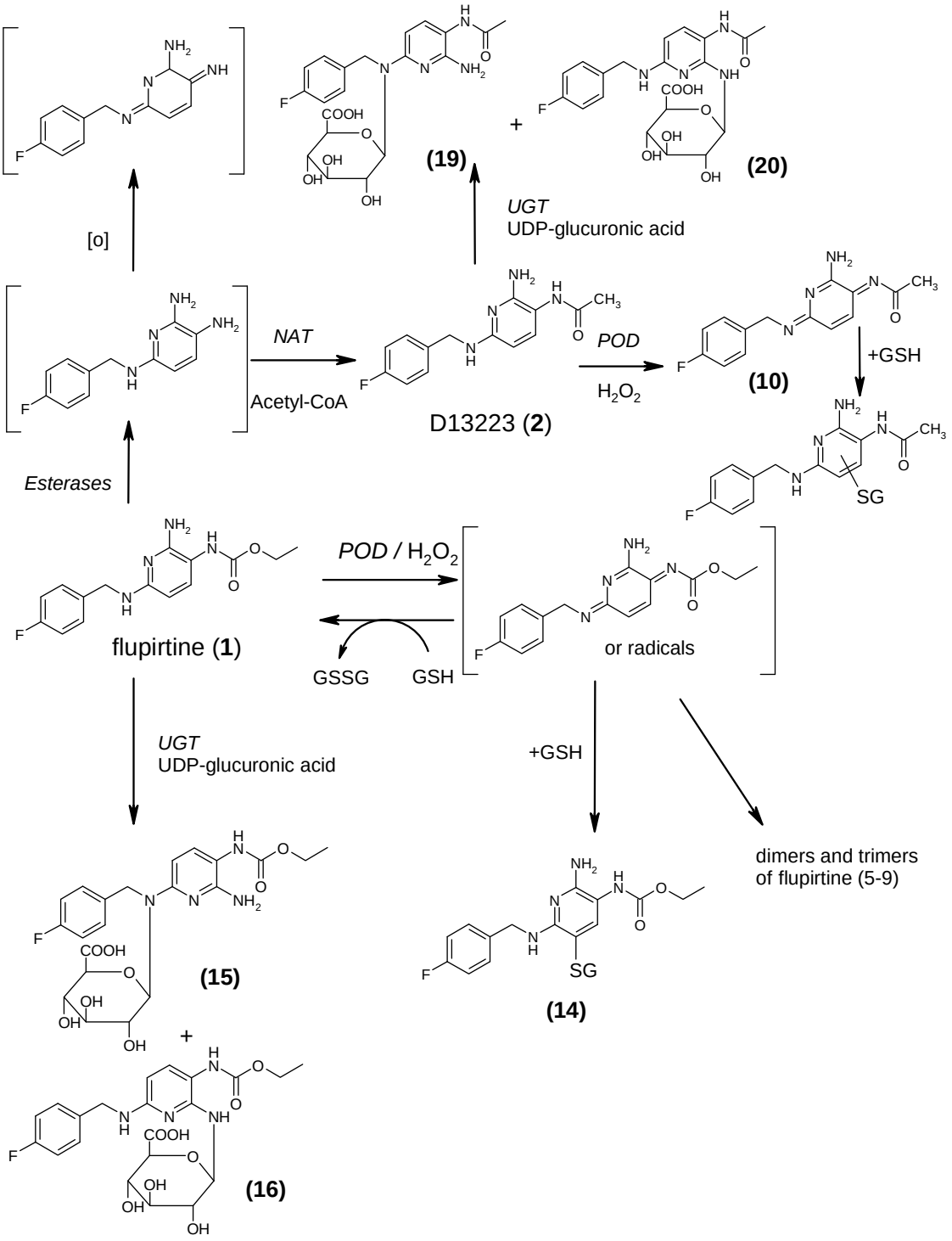

DMD Fast Forward. Published on December 12, 2008 as DOI: 10.1124/dmd.108.024364
This article has not been copyedited and formatted. The final version may differ from this version.

Figure 1

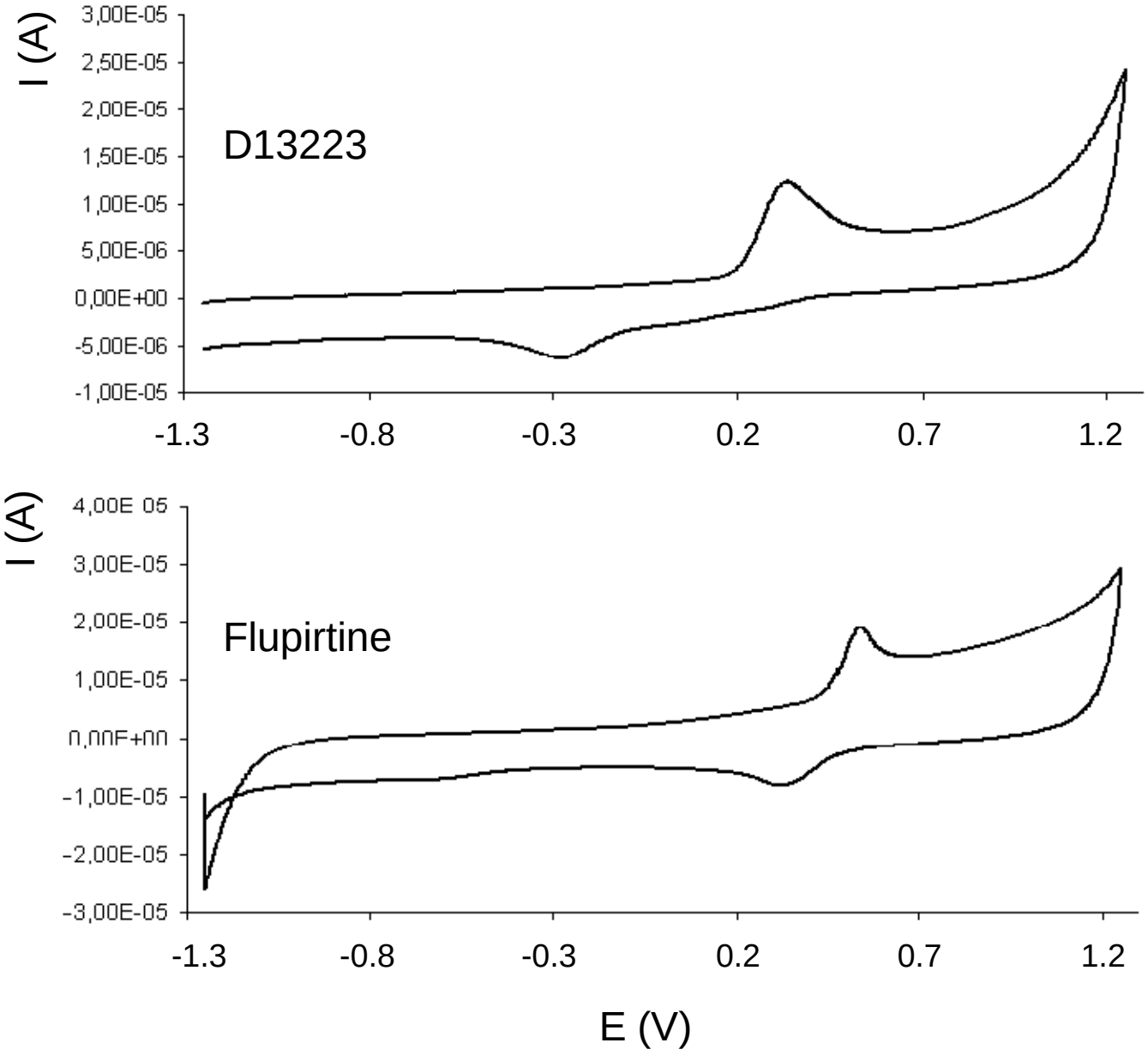

DMD Fast Forward. Published on December 12, 2008 as DOI: 10.1124/dmd.108.024364
This article has not been copyedited and formatted. The final version may differ from this version.

Figure 2.

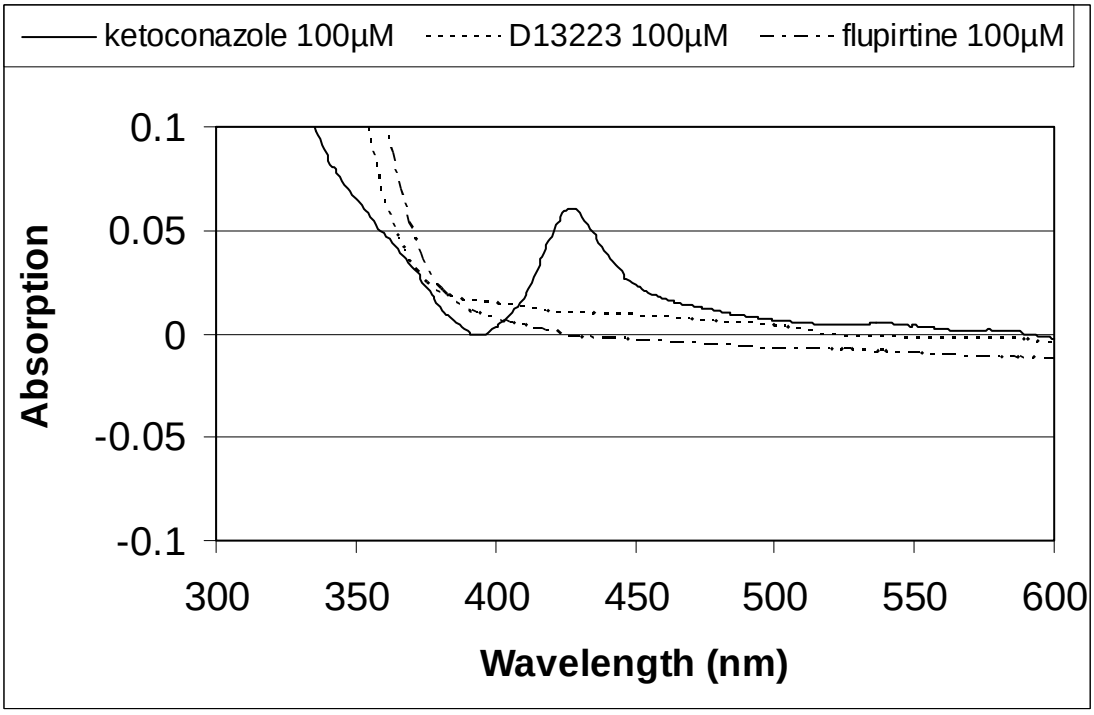

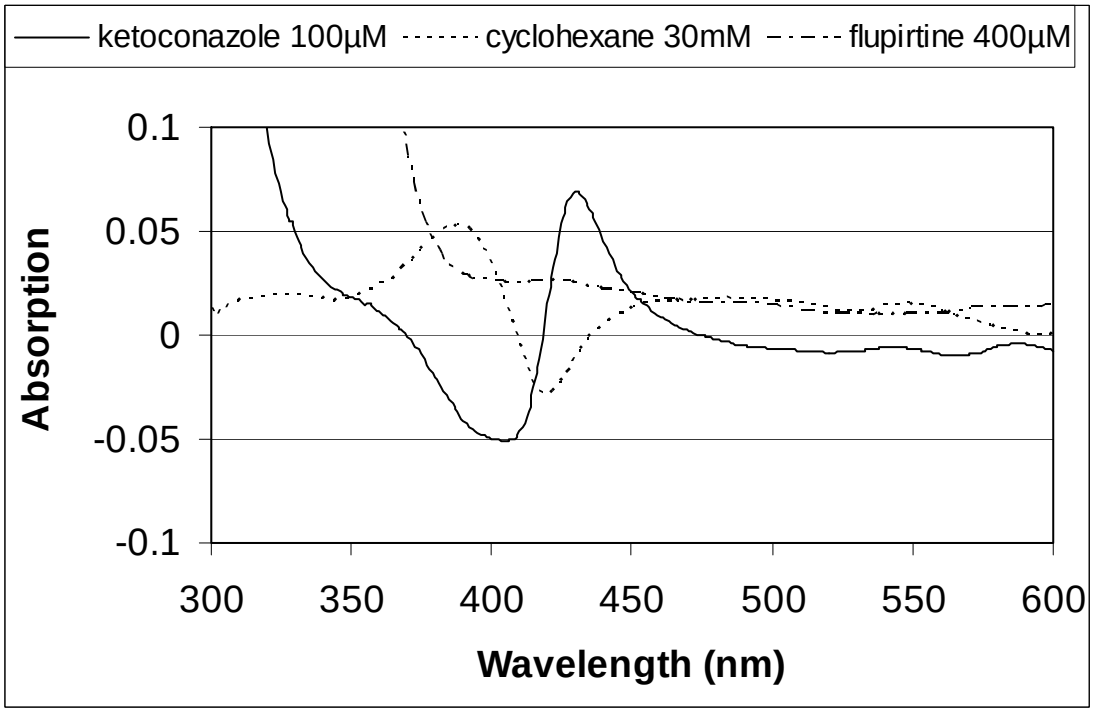

DMD Fast Forward. Published on December 12, 2008 as DOI: 10.1124/dmd.108.024364

Figure 3

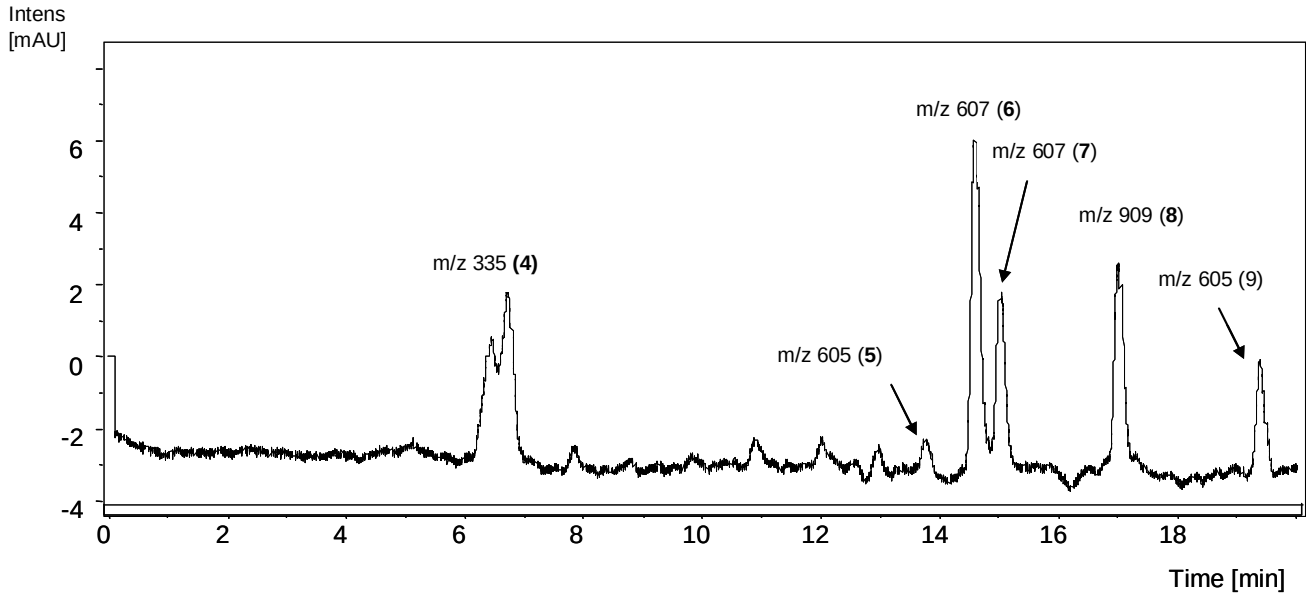

DMD Fast Forward. Published on December 12, 2008 as DOI: 10.1124/dmd.108.024364
This article has not been copyedited and formatted. The final version may differ from this version.

Figure 4

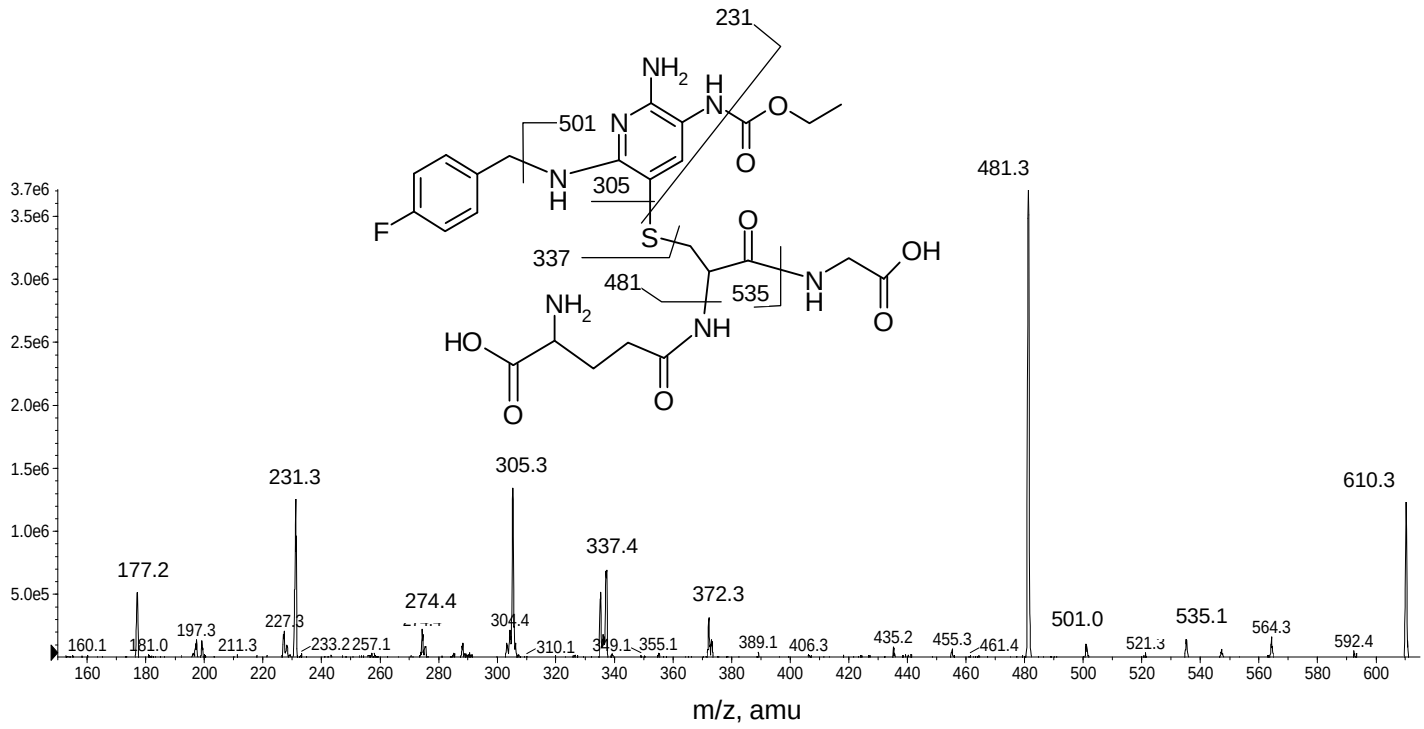

DMD Fast Forward. Published on December 12, 2008 as DOI: 10.1124/dmd.108.024364
This article has not been copyedited and formatted. The final version may differ from this version.

Figure 5

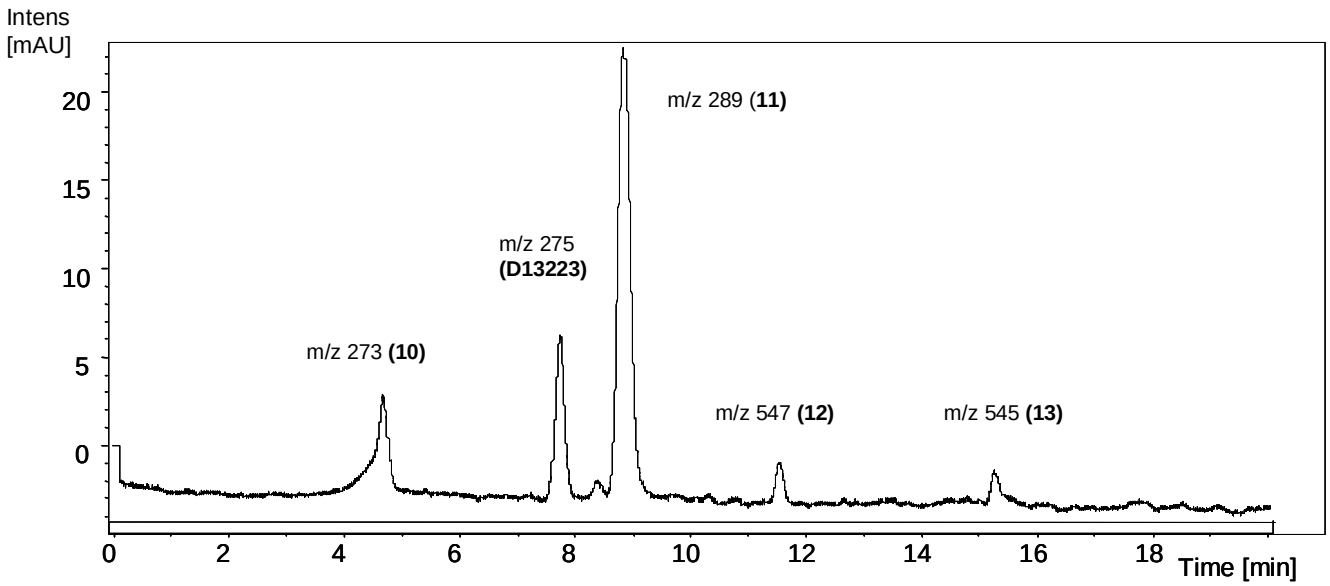

Figure 6

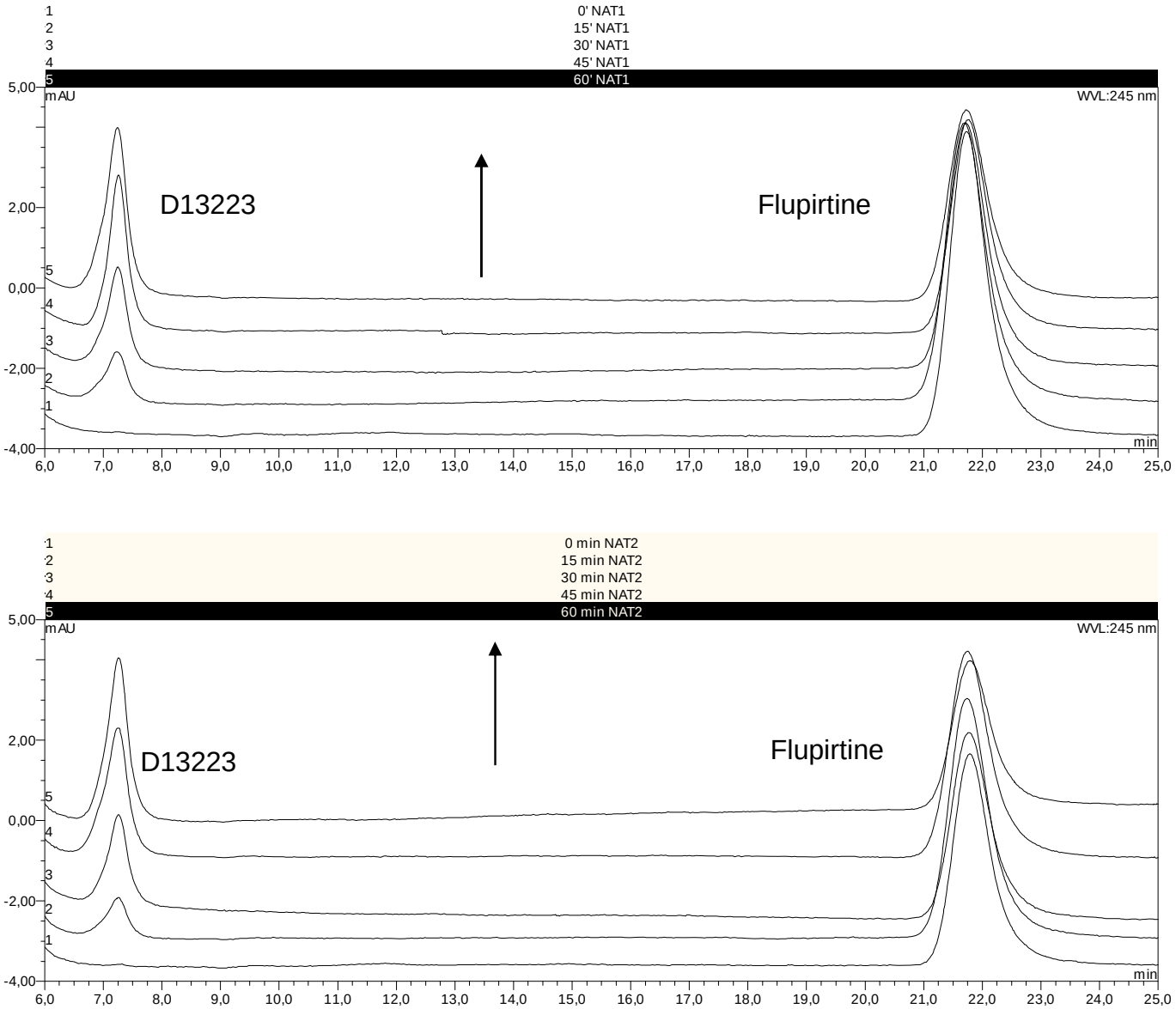

DMD Fast Forward. Published on December 12, 2008 as DOI: 10.1124/dmd.108.024364
This article has not been copyedited and formatted. The final version may differ from this version.

Figure 7

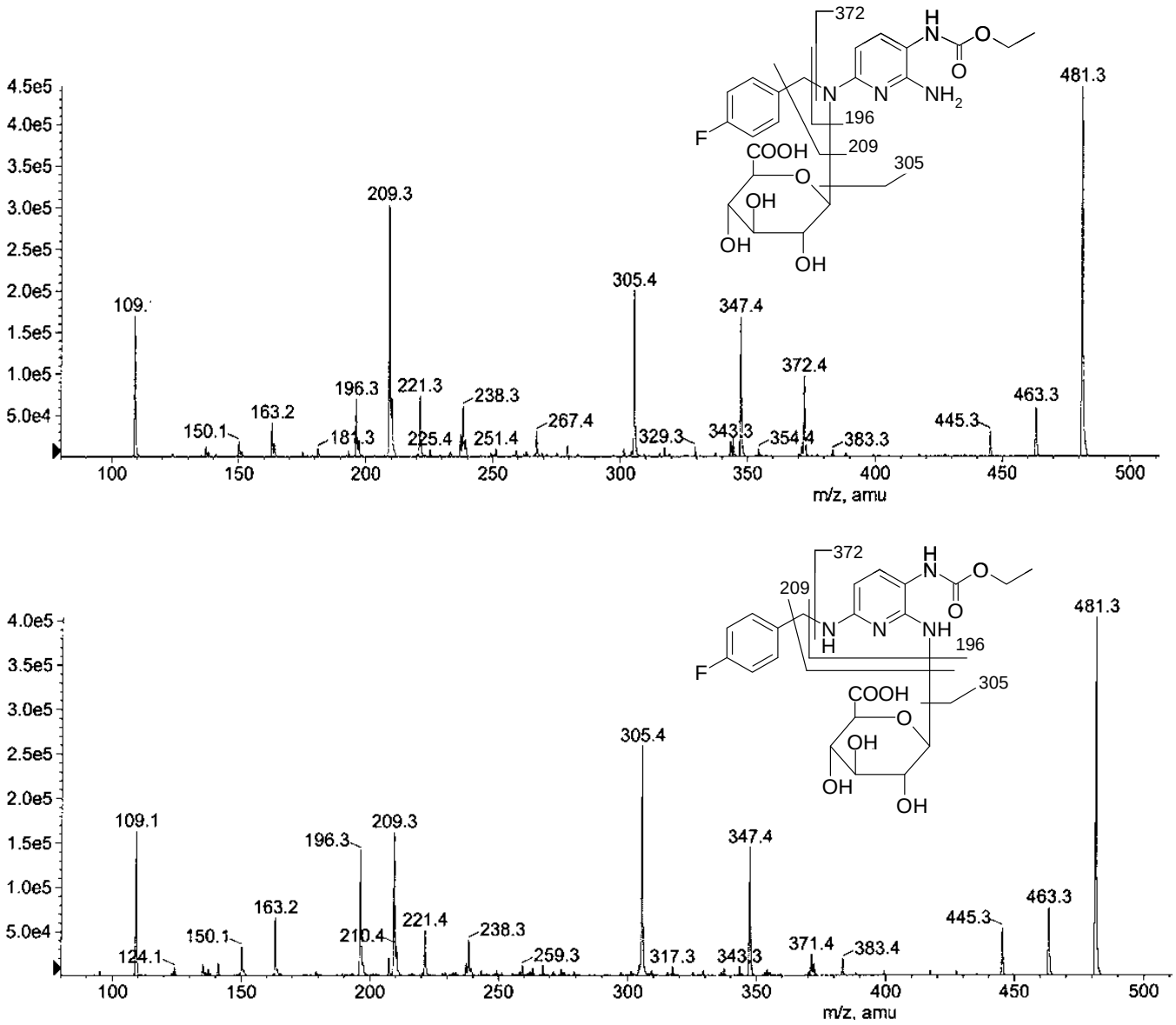

DMD Fast Forward. Published on December 12, 2008 as DOI: 10.1124/dmd.108.024364
This article has not been copyedited and formatted. The final version may differ from this version.

Figure 8